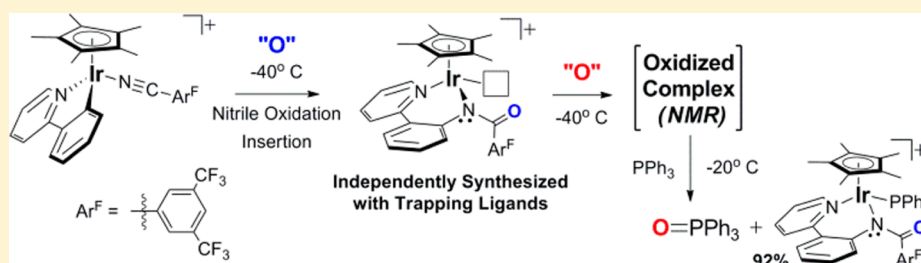


Oxygen Atom Transfer to a Half-Sandwich Iridium Complex: Clean Oxidation Yielding a Molecular Product

Christopher R. Turlington, Peter S. White, Maurice Brookhart, and Joseph L. Templeton*

W. R. Kenan Laboratory, Department of Chemistry, University of North Carolina at Chapel Hill, Chapel Hill, North Carolina 27599-3290, United States

S Supporting Information



ABSTRACT: The oxidation of $[\text{Ir}(\text{Cp}^*)(\text{phpy})(\text{NCAr}^{\text{F}})][\text{B}(\text{Ar}^{\text{F}})_4]$ (**1**; $\text{Cp}^* = \eta^5\text{-pentamethylcyclopentadienyl}$, $\text{phpy} = 2\text{-phenylene-}\kappa\text{C}1'\text{-pyridine-}\kappa\text{N}$, $\text{NCAr}^{\text{F}} = 3,5\text{-bis}(\text{trifluoromethyl})\text{benzonitrile}$, $\text{B}(\text{Ar}^{\text{F}})_4 = \text{tetrakis}[3,5\text{-bis}(\text{trifluoromethyl})\text{phenyl}]\text{-borate}$) with the oxygen atom transfer (OAT) reagent 2-*tert*-butylsulfonyliodosobenzene (sPhIO) yielded a single, molecular product at -40°C . New $\text{Ir}(\text{Cp}^*)$ complexes with bidentate ligands derived by oxidation of phpy were synthesized to model possible products resulting from oxygen atom insertion into the iridium–carbon and/or iridium–nitrogen bonds of phpy. These new ligands were either cleaved from iridium by water or formed unreactive, phenoxide-bridged iridium dimers. The reactivity of these molecules suggested possible decomposition pathways of $\text{Ir}(\text{Cp}^*)$ -based water oxidation catalysts with bidentate ligands that are susceptible to oxidation. Monitoring the $[\text{Ir}(\text{Cp}^*)(\text{phpy})(\text{NCAr}^{\text{F}})]^+$ oxidation reaction by low-temperature NMR techniques revealed that the reaction involved two separate OAT events. An intermediate was detected, synthesized independently with trapping ligands, and characterized. The first oxidation step involves direct attack of the sPhIO oxidant on the carbon of the coordinated nitrile ligand. Oxygen atom transfer to carbon, followed by insertion into the iridium–carbon bond of phpy, formed a coordinated organic amide. A second oxygen atom transfer generated an unidentified iridium species (the “oxidized complex”). In the presence of triphenylphosphine, the “oxidized complex” proved capable of transferring one oxygen atom to phosphine, generating phosphine oxide and forming an $\text{Ir}\text{-PPh}_3$ adduct in 92% yield. The final $\text{Ir}\text{-PPh}_3$ product was fully characterized.

INTRODUCTION

Isolated terminal oxo complexes of the late transition metals (groups 9–11) are rare.¹ Despite being invoked as key intermediates in biological² and industrial³ processes, only two mononuclear examples exist: a $\text{Pt}^{\text{IV}}\text{-oxo}$ complex supported by a tridentate P–C–N pincer ligand^{4,5} and a (mesityl)₃ $\text{Ir}^{\text{V}}\text{-oxo}$ compound (Figure 1).^{6,7} A bridging oxo ligand in a dinuclear iridium species also exhibits an unusually short iridium–oxygen bond distance (1.858 Å) and may be considered a third example of a late-transition-metal–oxo complex.⁸ Notably, reports of oxo complexes of gold,⁹ platinum,¹⁰ and palladium,¹¹ stabilized by polyoxometalate ligands, have recently been retracted due to misidentification of the metal in the metal–oxo bond.¹²

Iridium complexes that serve as precursors for water oxidation catalysts have been intensely studied,^{13–19} and $\text{Ir}^{\text{V}}\text{-oxo}$ complexes were originally invoked as reactive intermediates.^{20,21} However, these iridium catalysts, often possessing a Cp^* ligand and a κ^2 chelating ligand in the coordination sphere, have been plagued by oxidative ligand degradation under the

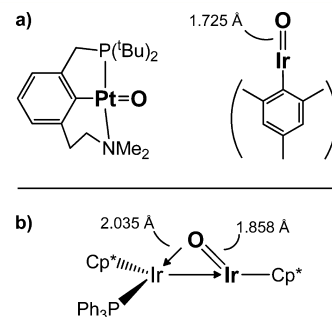
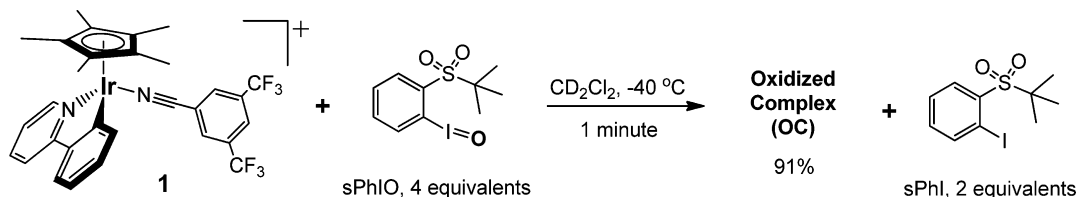


Figure 1. (a) Late-transition-metal–oxo complexes. (b) An asymmetric bridging oxo ligand with an unusually short iridium–oxygen bond length.

harsh oxidizing conditions required for water oxidation.^{22–25} Reports implicate degradation to iridium-based nanoparticles

Received: December 21, 2013

Published: February 26, 2014

Scheme 1. Low-Temperature Oxidation of **1** with sPhIO

(IrO_x·*n*H₂O is a known water oxidation catalyst)^{26,27} when using either ceric ammonium nitrate or electrochemical methods for oxidation.^{28,29} Systems employing sodium periodate, a less harsh oxidant, have achieved molecular water oxidation³⁰ and C–H activation,^{31–33} yet even in this system Cp* ligand oxidation and loss is observed.^{34,35} For molecular catalysts using sodium periodate as oxidant, nucleophilic attack on a terminal iridium–oxo moiety has been suggested as an explanation for the observed catalyst activity.^{36–38} Despite much effort, no experimental evidence for Cp*Ir^V–oxo complexes has been reported.

Recently we reported low-temperature oxidations of [Ir(Cp*)(ppy)(NCAR^F)] [B(Ar^F)₄] (**1**; Cp* = η⁵-pentamethylcyclopentadienyl, ppy = 2-phenylene-κC^{1'}-pyridine-κN, NCAR^F = 3,5-bis(trifluoromethyl)benzotrile, B(Ar^F)₄ = tetrakis[3,5-bis(trifluoromethyl)phenyl]borate), a complex related to numerous water oxidation catalysts, with the oxygen atom transfer (OAT) reagents iodosobenzene (PhIO) and dimethyldioxirane (DMDO).³⁹ Oxidation with PhIO and DMDO resulted in decomposition of **1**, rather than oxidation of the metal to form an Ir^V–oxo moiety.

In an extension of this work, we discovered that the OAT reagent 2-tert-butylsulfonyliodosobenzene (sPhIO),^{40–42} a more soluble analogue of PhIO, reacted cleanly with **1** at low temperatures. A single product was generated, and Cp* degradation was not implicated. Reaction with HCl led to an Ir(III) product reflecting insertion into the Ir–C bond of the ppy ligand. Insertion follows oxidation of an electron-deficient nitrile ligand, and an intermediate has been identified and prepared independently. Although the final low-temperature metal-based oxidation product could not be isolated, introducing triphenylphosphine yielded triphenylphosphine oxide and an Ir–PPh₃ adduct in 92% yield. Experimental evidence implicating a high-valent Ir^V–oxo monomer remains elusive.

RESULTS AND DISCUSSION

Low-Temperature Oxidation with the Soluble Iodosoaryl Reagent 2-tert-Butylsulfonyliodosobenzene (sPhIO). When complex **1** was treated with 4 equiv of the OAT reagent sPhIO at -40 °C in dichloromethane-*d*₂, 91% conversion (based on an internal standard) to a new, temperature-sensitive iridium species was observed by ¹H NMR spectroscopy (Scheme 1). Two equivalents of 2-tert-butylsulfonyliodobenzene (sPhI, the reduced oxidant) was also generated, indicating *two* oxygen atom transfers per iridium. The reaction did not reach full conversion unless excess oxidant was used, presumably due to the limited solubility of iodonium ylides⁴⁰ and slow second-order kinetics as the reagent concentrations dwindled.

The reactive oxidized complex (OC) could only be characterized by low-temperature NMR spectroscopy, and this complex displayed ¹H NMR resonances for Cp* and ppy that were clearly distinct from those of **1** (Figure 2). Upon

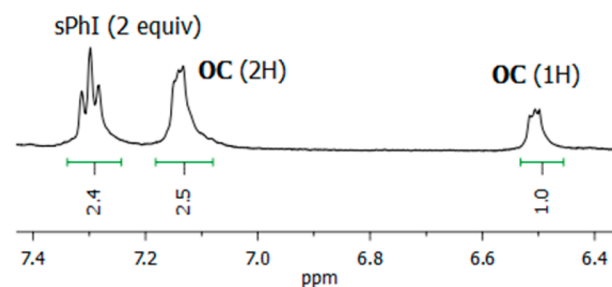
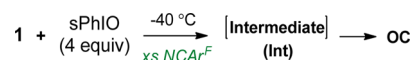


Figure 2. Expansion of the aromatic region of the ¹H NMR spectrum of the OC at -40 °C. When the OC is formed from oxidation of **1** with excess sPhIO, 2 equiv of sPhIO is generated relative to the OC.

oxidation, the Cp* methyl resonance (singlet, 15H) shifted dramatically upfield from 1.68 to 1.24 ppm, and one of the ppy proton resonances shifted at least 0.5 ppm upfield to 6.48 ppm (no ppy proton resonance appeared upfield of 7.11 ppm in **1**). Importantly, the NCAR^F moiety was still present in the coordination sphere (the ¹H chemical shifts observed for the nitrile ligand did not correspond to those of the free ligand). At -70 °C, the ¹H NMR spectrum of the OC decoalesced into two isomers (see the Supporting Information).⁴³ Isomers could result from restricted rotation of the aryl–pyridine bond of a new κ² ligand, arising from structural modification of the ppy ligand upon oxidation. Samples of the OC were unstable above -20 °C, at which temperature the oxidized complex began decomposing and reacting with excess sPhIO. Oxidation at temperatures higher than -20 °C led to intractable materials; the resulting NMR spectra were complicated and suggested ligand oxidation and degradation.²⁸ Despite utilizing low-temperature column chromatography and low-temperature crystallization techniques, our efforts to isolate the OC proved unsuccessful.

When the oxidation of **1** was conducted in the presence of exogenous NCAR^F, an intermediate could be detected (Scheme 2).

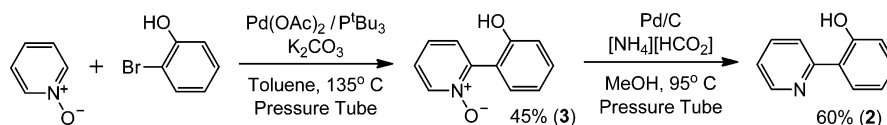
Scheme 2. Observation of an Intermediate (Int) in the Presence of Excess Nitrile during Formation of the OC



The intermediate (Int) had chemical shifts in the aromatic region similar to those of the OC, suggesting that modification of the ppy ligand had occurred in a previous step. The Int cleanly converted to the OC over time at -40 °C in the presence of sPhIO. Presumably, added NCAR^F trapped an iridium species with a vacant coordination site, which allowed observation of the transient Int. In the absence of trapping ligand, the unsaturated iridium species reacted too quickly to be observed by low-temperature NMR spectroscopy.

Complexes Representing Oxygen Atom Insertion Products. When attempts to isolate the OC failed, the

Scheme 3. Synthesis of Proligands 2 and 3

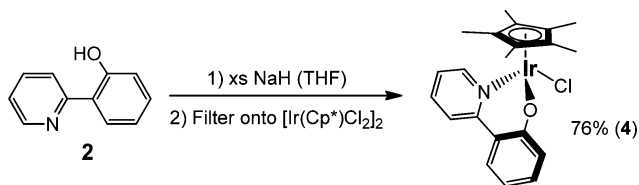


synthesis of potential oxidation products was pursued. Inspired by reports of olefin insertion into the iridium–carbon bond of $[\text{Ir}(\text{Cp}^*)(\text{phpy})(\text{olefin})]^+$ complexes,⁴⁴ we hypothesized that oxygen atom insertion into either the iridium–carbon or the iridium–nitrogen bond of phpy was possible. To investigate this possibility, we independently prepared complexes exhibiting such structural features.

A proligand that could serve as a model for oxygen atom insertion into the iridium–carbon bond of phpy, 2-(2-hydroxyphenyl)pyridine (2), has been reported.⁴⁵ A different synthetic route to 2 was employed to also allow access to a phpy-derived ligand representing oxygen atom insertion into both the iridium–carbon and iridium–nitrogen bonds. The proligand 2-(2-hydroxyphenyl)pyridine *N*-oxide (3) was synthesized in one step using a modified coupling procedure (Scheme 3).^{46,47} Acceptable yields were achieved when the reaction solution was heated above the boiling point of the solvent (toluene) in a closed reaction vessel. Employing lower temperatures resulted in lower yields and only partial conversion of the 2-bromophenol substrate. The yield for this reaction was low in comparison to other coupling reactions reported for pyridine *N*-oxides and bromoarenes.⁴⁶ This is likely due to the properties of the 2-bromophenol reagent, which is sterically demanding and can also bind to the metal as a phenoxide ligand.⁴⁸ Reduction of 3 to the known compound 2 required conditions more forcing than expected for reduction of *N*-oxides.⁴⁶ Full conversion could be achieved when 3 was heated at reflux for 48 h in the presence of ammonium formate and Pd/C. It may be that the *N*-oxide of 3 is stabilized by hydrogen bonding to the phenolic hydrogen, which lowers its reactivity.

Metalation of 2 was accomplished following deprotonation of the proligand by an insoluble base (NaH) in THF. This solution was filtered by cannula directly into a vessel with $[\text{Ir}(\text{Cp}^*)\text{Cl}_2]_2$ (Scheme 4). The sodium ion from the salt of

Scheme 4. Metalation of 2, Yielding Complex 4



deprotonated 2 abstracted 1 equiv of chloride from the iridium, thus allowing κ^2 coordination of the ligand. The iridium product, $\text{Ir}(\text{Cp}^*)(2\text{-}(2\text{-pyridyl})\text{phenoxide})\text{Cl}$ (4), was stable to both moisture and air and could be conveniently purified by chromatography on silica.

The X-ray structure of 4 was obtained and is shown in Figure 3. The aromatic rings of the bound chelating ligand 2 are canted by 27.9°. The constraint imposed on the conjugated aryl system is the consequence of forming a six-membered metallacycle. Both the iridium–oxygen bond distance (2.082 Å) and the iridium–nitrogen bond distance (2.100 Å) were within expected bonding distances for iridium complexes.^{49–51}

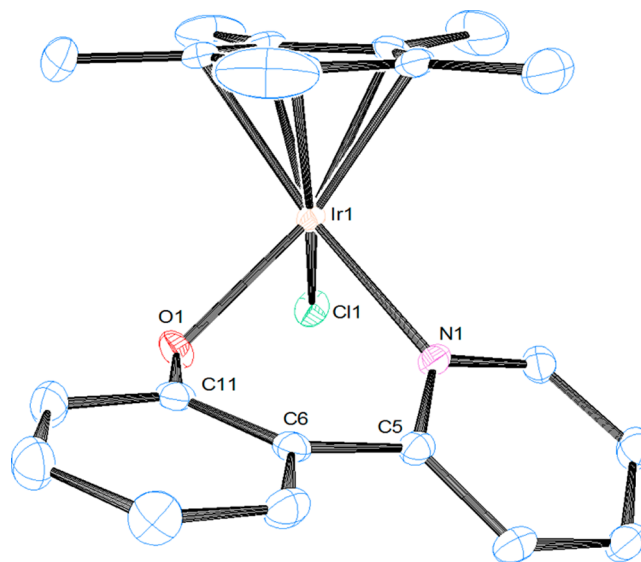
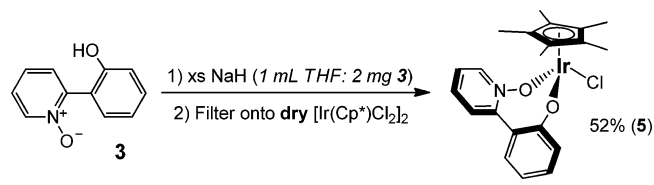


Figure 3. ORTEP drawing of 4, with partial numbering scheme (50% probability thermal ellipsoids). Hydrogen atoms are omitted for clarity. Selected bond lengths (Å), bond angles (deg), and torsion angles (deg): Ir₁–O₁ 2.082(2), Ir₁–N₁ 2.100(3), Ir₁–Cl₁ 2.4070(8), C₁₁–O₁ 1.325(4); O₁–Ir₁–Cl₁ 85.81(7), N₁–Ir₁–O₁ 82.74(10), Cl₁–Ir₁–N₁ 86.28(7), Ir₁–O₁–C₁₁ 114.34(19); C₁₁–C₆–C₅–N₁ 27.9(5).

Metalation of 3 was more challenging because of the poor solubility of the pyridine *N*-oxide.⁴⁶ It was necessary to use at least 1 mL of THF for every 2 mg of proligand to ensure complete dissolution of the sodium salt of 3. When this ratio of THF to 3 was used, deprotonation of the phenol by NaH and cannula filtration onto $[\text{Ir}(\text{Cp}^*)\text{Cl}_2]_2$ yielded $\text{Ir}(\text{Cp}^*)(2\text{-}(2\text{-pyridyl})\text{phenoxide } N\text{-oxide})\text{Cl}$ (5; Scheme 5). The $[\text{Ir}(\text{Cp}^*)\text{Cl}_2]_2$

Scheme 5. Metalation of 3, Yielding Complex 5



dimer had to be carefully dried by heating to 50 °C under high vacuum overnight. This prevented protonation of the sodium salt of 3 prior to reaction with the metal. In addition, the product displayed extreme sensitivity to moisture. Product instability will be discussed later.

The growth of crystals of 5 was accomplished by preparing a saturated solution of the complex in pentane and storing in a glovebox freezer at –25 °C. Structural characterization of 5 represents a rare example of an iridium complex with a bound *N*-oxide (Figure 4).^{52,53} The iridium–oxygen bond length of the coordinated *N*-oxide is 2.111 Å, which is comparable to the rhodium–oxygen bond length of a coordinated pyridine *N*-oxide (2.080 Å) in a $[\text{Rh}(\text{cycloocta-1,5-diene})(\mu\text{-pyridinyl } N\text{-oxide})]_2$

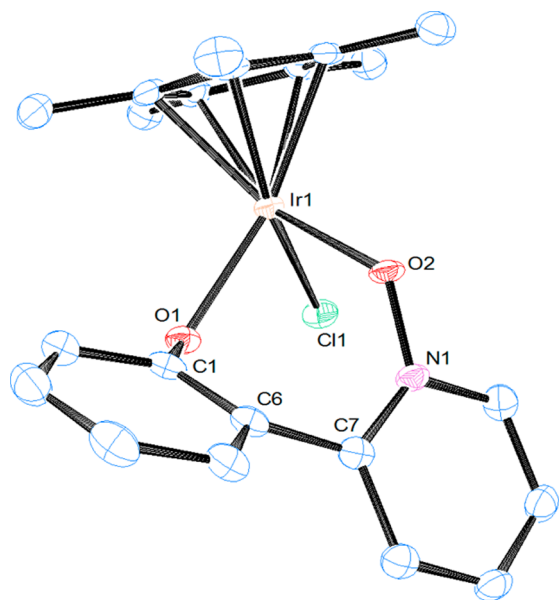


Figure 4. ORTEP drawing of **5**, with partial numbering scheme (50% probability thermal ellipsoids). Hydrogen atoms are omitted for clarity. Selected bond lengths (Å), bond angles (deg), and torsion angles (deg): Ir₁–O₁ 2.101(2), Ir₁–O₂ 2.111(2), Ir₁–Cl₁ 2.4130(7), C₁–O₁ 1.338(4), O₂–N₁ 1.350(3); O₁–Ir₁–Cl₁ 83.59(6), O₂–Ir₁–O₁ 82.44(8), Cl₁–Ir₁–O₂ 91.67(6), Ir₁–O₁–C₁ 119.64(19), Ir₁–O₂–N₁ 123.36(17); C₁–C₆–C₇–N₁ 51.3(4).

dimer (the analogous distances in the two reported square-planar Ir(I) complexes were 2.031 and 2.030 Å).⁵⁴ The octahedral geometry of **5** and the seven-membered metallacycle with a coordinated *N*-oxide are unique for iridium. The seven-membered metallacycle forces the two aryl rings to deviate from planarity by a remarkable 51.3°, a phenomenon that has also been reported in metal complexes with the isoelectronic κ^2 chelating ligand 2,2'-bipyridine *N,N'*-dioxide.⁵⁵ The Ir–Oph bond distance is 2.101 Å, which is comparable to the analogous distance in **4**.

Reactivity of Complexes with Oxidized phpy Ligands and Implications for Catalyst Degradation. The neutral iridium chloride complexes **4** and **5** were distinct from the OC, because the OC included a nitrile ligand. Replacement of the chloride ligand by NCAR^F in complex **4** was attempted by combining Na[B(Ar^F)₄] and **4** in the presence of NCAR^F. A new iridium complex was formed after 24 h, but surprisingly, the nitrile ligand was not coordinated. X-ray diffraction analysis on a suitable crystal revealed the dinuclear iridium product [Ir(Cp*)(2-(2-pyridyl)- μ -phenoxide)]₂[B(Ar^F)₄]₂ (**6**), with bridging phenoxide ligands (Figure 5). The structure of **6** showed an elongated carbon–oxygen bond of 1.361 Å (for comparison, the same bond in **4** is 1.325 Å). The Ir₂O₂ core was roughly planar, and the iridium nuclei do not interact, as they are separated by 3.441 Å. Remarkably, the Cp* methyl protons resonated at 0.59 ppm in the ¹H NMR spectrum, which is an upfield shift of greater than 0.7 ppm from the starting material **4**. This shift is likely accounted for by the Cp* methyl groups being positioned within the shielding region of the arylpyridine ligands. In the absence of the benzonitrile ligand, **6** was formed in several hours. Dimer **6** was not sensitive to air or moisture, and a 21 h exposure to either carbon monoxide or ethylene failed to cleave the dimer into mononuclear components (Scheme 6). If oxygen atom

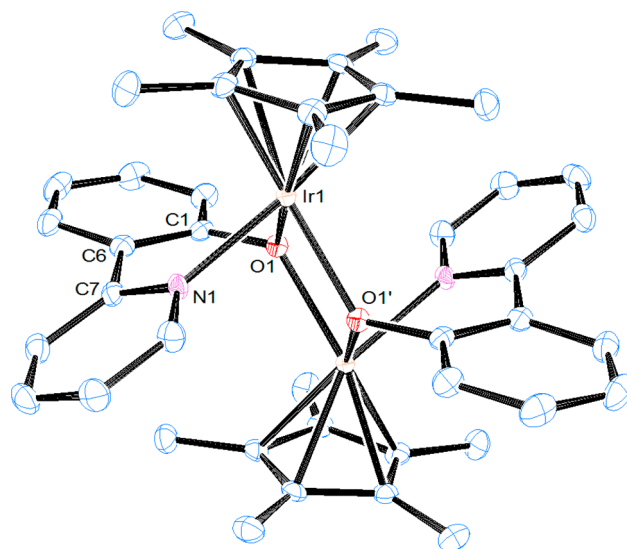
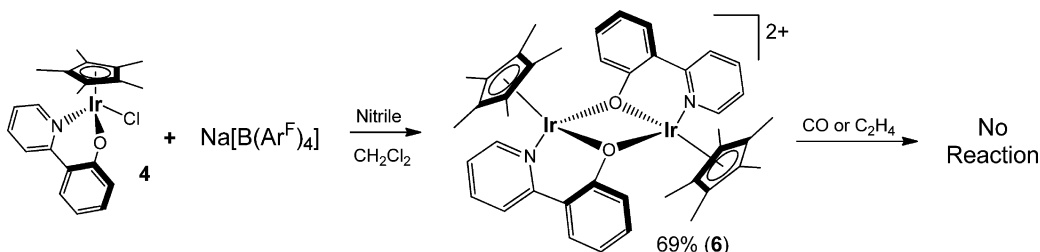


Figure 5. ORTEP drawing of **6**, with partial numbering scheme (50% probability thermal ellipsoids). The anions and hydrogen atoms are omitted for clarity. Selected bond lengths (Å), bond angles (deg), and torsion angles (deg): Ir₁–O₁ 2.1294(17), Ir₁–O₁' 2.1373(17), Ir₁–N₁ 2.099(2), C₁–O₁ 1.361(3); O₁–Ir₁–O₁' 72.49(7), O₁'–Ir₁–N₁ 80.12(7), N₁–Ir₁–O₁ 80.96(7), Ir₁–O₁–Ir₁' 107.51(7); C₁–C₆–C₇–N₁ 31.4(4).

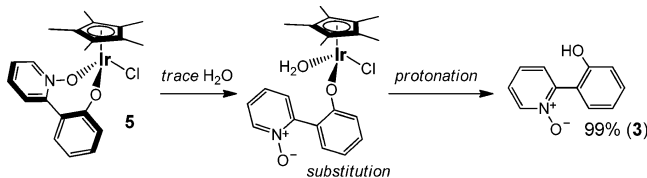
insertion into the iridium–carbon bond of a bidentate ligand is possible, formation of **6** could represent an example of a deactivation pathway implicating a bidentate ligand in an Ir(Cp*) water oxidation catalyst. Many studies citing catalyst decomposition propose Cp* degradation pathways,^{22–25,34,35} but the role of the bidentate ligand is not clear. Complexes that are known to be molecular catalysts when driven by the sacrificial oxidant NaIO₄ include bidentate ligands with pyridine ligands or propanolate ligands, which are less likely to facilitate oxygen atom insertion than an iridium–carbon bond.^{30,34}

As mentioned earlier, **5** is sensitive to water. When 2.0 μ L of water (0.11 mmol) was added to a solution of **5** (6.5 mg, 0.012 mmol) in dry dichloromethane-*d*₂, the ¹H NMR resonances of **5** disappeared after 1 min of vigorous shaking. One product of decomposition was the protonated proligand **3**, which was identified in the ¹H NMR spectrum (99% conversion, on the basis of an internal standard). The sensitivity of **5** to water may arise from the weak bonding interaction between the hard pyridine *N*-oxide donor ligand and iridium. Substitution of water for the pyridine *N*-oxide, therefore, would result in κ^1 coordination of the 2-(2-pyridyl)phenoxide *N*-oxide ligand (Scheme 7). Protonation of the phenoxide-bound ligand **3** is attractive as the second step leading toward cleavage of **3** from iridium. Water molecules coordinated to metals are acidic ($pK_a < 10$) and could serve as the proton donor.⁵⁶ Loss of the oxidized ligand **3** demonstrates that a modified bidentate ligand may be cleaved from Ir(Cp*) complexes. The final identity of the iridium product formed from **5** and water has not been determined, but it may be an [Ir(Cp*)(OH)Cl]_{*n*} species. Formation of a water-sensitive seven-membered metallacycle by oxygen atom insertion into both the iridium–carbon and the iridium–nitrogen bonds is an improbable decomposition pathway for molecular iridium species involving bidentate ligands, since oxygen atom insertion into an iridium–nitrogen bond is unprecedented. None of the independently synthesized iridium complexes prepared with oxidized phpy ligands were

Scheme 6. Formation of 6 and Reaction with Trapping Ligands



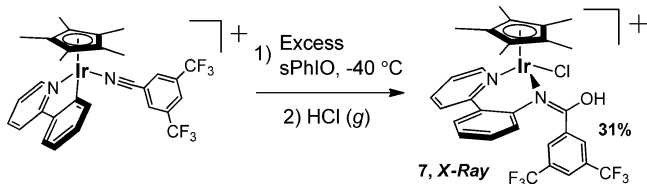
Scheme 7. Proposed Reaction of 5 with Water



identical with the OC, as assessed by ¹H NMR spectroscopy. However, their properties and behavior yielded insights into potential decomposition pathways involving phpy ligands in water oxidation catalysts.

Reaction of the Oxidized Complex with HCl. When independent synthesis failed to illuminate the identity of the OC, efforts were made to cleave the modified phpy ligand from the OC and characterize it. Accordingly, HCl(g) was purged through a freshly prepared sample of the OC in dichloromethane-*d*₂ at -40 °C. This led to a new iridium product with the Cp*, nitrile, and phenylpyridine ligand components within the coordination sphere (Scheme 8). In addition, HCl reacted

Scheme 8. Treatment of the OC with HCl, Forming 7



with excess sPhIO (presumably forming sPhIO₂, a milder oxidant),⁵⁷ which slowed decomposition of the iridium complex when the sample was warmed. After the samples of the OC treated with HCl were warmed to room temperature, the reaction mixture was washed with water, and the solvent (dichloromethane) was removed in vacuo. Residual sPhI was removed by washing the solids copiously with pentane, and crystals suitable for X-ray analysis were grown by layering pentane on top of a concentrated solution of the metal species in dichloromethane. The molecular structure revealed the iridium product as [Ir(Cp*)(3,5-bis(trifluoromethyl)-*N*-(2-(2-pyridyl)phenyl)benziminol)Cl][B(Ar^F)₄] (7; Figure 6). Notably, the nitrile had inserted into the iridium–carbon bond of phpy and the original nitrile carbon now possessed a hydroxyl group. The new iminol moiety was verified by the bond lengths reported in the structure. The C–N bond length was 1.294 Å, and the C–O bond length was 1.316 Å, verifying the identity of the imine C=N and C–O bonds of 7, respectively. In addition, the torsion angle between the two aryl rings of the modified phpy ligand (37.3°) was greater than the torsion angles

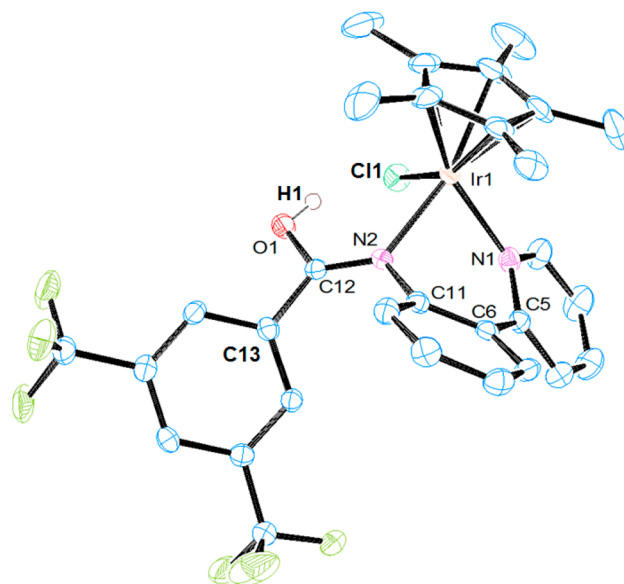
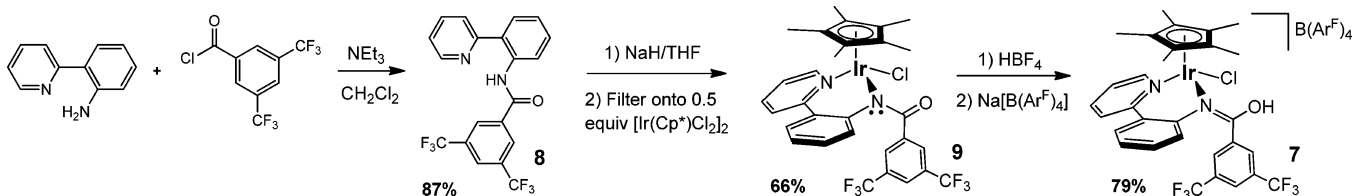


Figure 6. ORTEP drawing of 7, with partial numbering scheme (50% probability thermal ellipsoids). The anion and all hydrogen atoms except the alcohol OH are omitted for clarity. Selected bond lengths (Å), bond angles (deg), and torsion angles (deg): Ir₁–Cl₁ 2.4035(7), Ir₁–N₁ 2.109(2), Ir₁–N₂ 2.123(2), N₂–C₁₂ 1.294(4), N₂–C₁₁ 1.441(4), O₁–C₁₂ 1.316(4); Ir₁–N₂–C₁₂ 128.22(19), C₁₁–N₂–C₁₂ 121.7(2), N₂–C₁₂–O₁ 121.7(3), N₂–C₁₂–C₁₃ 126.8(3); C₁₁–C₆–C₅–N₁ 37.3(4).

between the aryl groups in the other six-membered metallocycles for complexes 4 (27.9°) and 6 (31.4°). The resonances in the ¹H NMR spectrum of 7 were similar to those observed for the OC, but in addition there appeared a broad singlet assigned to the alcohol OH at 12.1 ppm.

Synthesis of Complexes Relevant to Oxidation of 1.

The identities of the Int and OC were not apparent from the structural characterization of the HCl addition product 7. Only one oxygen atom was incorporated into the ligand framework of 7, while integration of sPhI after formation of the OC suggested that 2 equiv of oxygen atoms had been consumed. The identity of the sixth ligand in the Int and the OC was unknown, and chloride presumably displaced a ligand in the OC on the way to form 7. The new phpy-derived ligand in 7, however, appeared to be related to the phpy-derived ligands of the OC and Int, since the aromatic resonances in the ¹H NMR spectra of all three complexes included a characteristic resonance near 6.5 ppm. The resonance at 12.1 ppm for the hydroxyl proton only appeared upon treating the OC with HCl, which led us to believe that an amide was present in the OC, and furthermore, this amide reflected net insertion of an oxidized nitrile ligand under the oxidative conditions of the

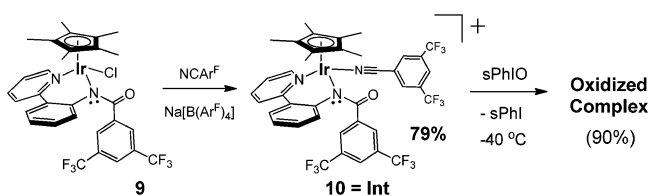
Scheme 9. Synthesis of Proligand **8** and Iridium Complexes Relevant to sPhIO Oxidation

reaction. Conversion of a coordinated amide to an iminol has been observed at iridium and other metals.⁵⁸

A proligand modeling the phpy-derived ligand corresponding to an amide was independently prepared. Synthesis of bis- CF_3 -substituted benzamide **8** was readily accomplished by an amide coupling reaction between 2-(2-pyridyl)aniline⁵⁹ and the commercially available 3,5-bis(trifluoromethyl)benzoyl chloride (Scheme 9). The conditions for the amide coupling followed a closely related procedure for the coupling of aminoquinolines and acid chlorides.⁶⁰

Metalation of **8** was accomplished using the same strategy as was used for metalation of proligands **2** and **3**. Proligand **8** was stirred over NaH in THF for 1.5 h and then filtered by cannula directly onto solid $[\text{Ir}(\text{Cp}^*)\text{Cl}_2]_2$ dimer (Scheme 9). The dimer was carefully dried by heating at 50 °C overnight under high vacuum. The product of metalation, $\text{Ir}(\text{Cp}^*)\{[(3,5\text{-bis}(\text{trifluoromethyl})\text{benzoyl})(2\text{-}(2\text{-pyridyl})\text{phenyl})\text{amide}]\text{Cl}\}$ (**9**), was stable to moisture and air, allowing for chromatography and purification on silica gel. Importantly, protonation of **9** with HBF_4 and counterion exchange with $\text{Na}[\text{B}(\text{Ar}^{\text{F}})_4]$ yielded **7**, which proved to be identical (as confirmed by NMR spectroscopy) with the species obtained when the OC reacted with HCl.

Identity of Intermediate. Substitution for the chloride ligand in **9** was achieved using $\text{Na}[\text{B}(\text{Ar}^{\text{F}})_4]$ in the presence of NCAr^{F} , yielding $[\text{Ir}(\text{Cp}^*)\{[(3,5\text{-bis}(\text{trifluoromethyl})\text{benzoyl})(2\text{-}(2\text{-pyridyl})\text{phenyl})\text{amide}]\text{NCAr}^{\text{F}}\}][\text{B}(\text{Ar}^{\text{F}})_4]$ (**10**; Scheme 10).

Scheme 10. Synthesis and Oxidation of **10**

^1H NMR spectral signals for **10** at -40 °C matched the ^1H NMR resonances observed for the **Int** formed in the reaction of **1**, sPhIO, and excess NCAr^{F} at -40 °C. Specifically, the Cp^* methyl groups (15H) of **10** resonated at 1.42 ppm at low temperature, while the same signal for the **Int** resonated at 1.45 ppm. The ^1H NMR spectrum of **10** also revealed doublets at 8.66 ppm ($J = 5.5$ Hz) and 6.51 ppm ($J = 7.5$ Hz), which matched well with doublets identified for the **Int** at 8.70 ppm ($J = 5.5$ Hz) and 6.52 ppm ($J = 8.0$ Hz). Furthermore, two triplets in the ^1H NMR spectrum of **10** (7.41 ppm, $J = 6.5$ Hz; 7.04 ppm, $J = 7.0$ Hz) were equivalent to two triplets observed for the **Int** (7.47 ppm, $J = 6.5$ Hz; 7.07 ppm, $J = 7.0$ Hz). Good agreement between the two ^1H NMR spectra at -40 °C convinced us that independently prepared complex **10** was in fact the **Int** observed under oxidative conditions in the presence of exogenous NCAr^{F} .

The reaction of **10** with sPhIO at -40 °C was also conducted. The oxidation reaction starting from **10** cleanly generated the OC in 90% yield (based on an internal standard) after 4 min of stirring at -40 °C. Importantly, only 1 equiv of sPhI was generated (Figure 7), further establishing the identity of **10** as

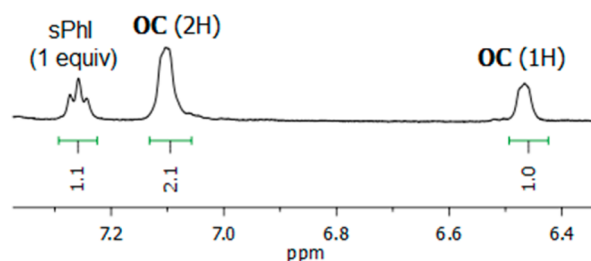
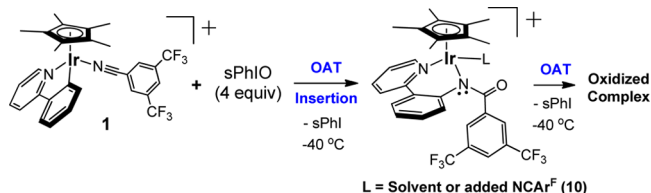


Figure 7. Expansion of the aromatic region of the ^1H NMR spectrum of the OC at -40 °C. When the OC is formed by oxidation of the isolated intermediate **10** with sPhIO, only 1 equiv of sPhI is generated.

the **Int** observed in the oxidation of **1** in the presence of excess NCAr^{F} . Excess sPhIO was again required for full conversion of the intermediate **10** to the OC. Note that intermediate **10** is not observed in the oxidation reaction of **1** with sPhIO in the absence of NCAr^{F} . In this case, the intermediate species is not stabilized by added trapping ligands, although it may be stabilized by interaction with the solvent (dichloromethane- d_2).

Neither complex **9** nor **10** exhibited dynamic behavior at -70 °C in their ^1H NMR spectra (the OC decoalesced into two isomers at this temperature). That single isomers were observed by ^1H NMR spectroscopy at -70 °C for complexes **9** and **10** possibly indicates that further modification of the κ^2 chelating ligand occurred upon oxidation of the **Int**.

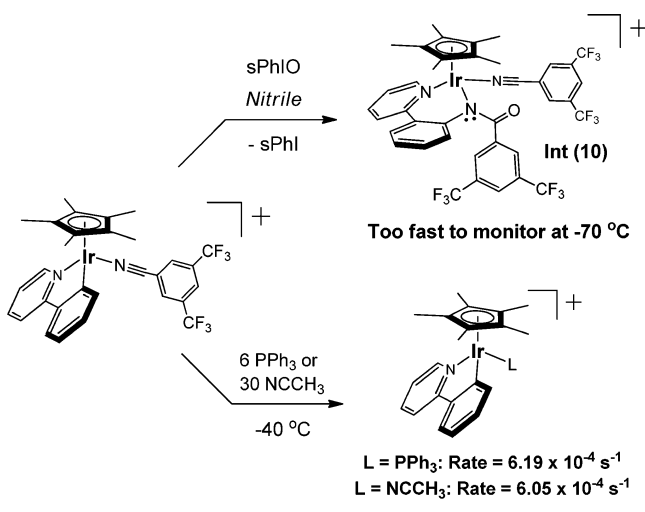
Mechanisms of First and Second Oxidation Steps. Following identification of the **Int** as **10**, independent synthesis of **10** allowed the individual oxidation steps to be studied in greater detail. These individual steps in the overall reaction of **1** with sPhIO are described in Scheme 11. Initial OAT to **1** results

Scheme 11. Individual Steps in the Oxidation of **1** with sPhIO

in oxidation of NCAr^{F} and insertion into the iridium–carbon bond of phpy, forming an amide. A second OAT step follows, and this step converts the intermediate to the OC and is accompanied by the generation of the second equivalent of sPhI.

Mechanism of Nitrile Oxidation in the First Oxidation Step. The kinetics of the first oxidation step were studied to determine if dissociation of the nitrile ligand was a prerequisite for nitrile oxidation. When a 6.3 mM solution of **1** with 6 equiv of sPhIO was mixed at $-70\text{ }^{\circ}\text{C}$, the first oxidation step was too fast to monitor by ^1H NMR spectroscopy, both in the absence and in the presence of 44 equiv of NCAr^{F} (Scheme 12).

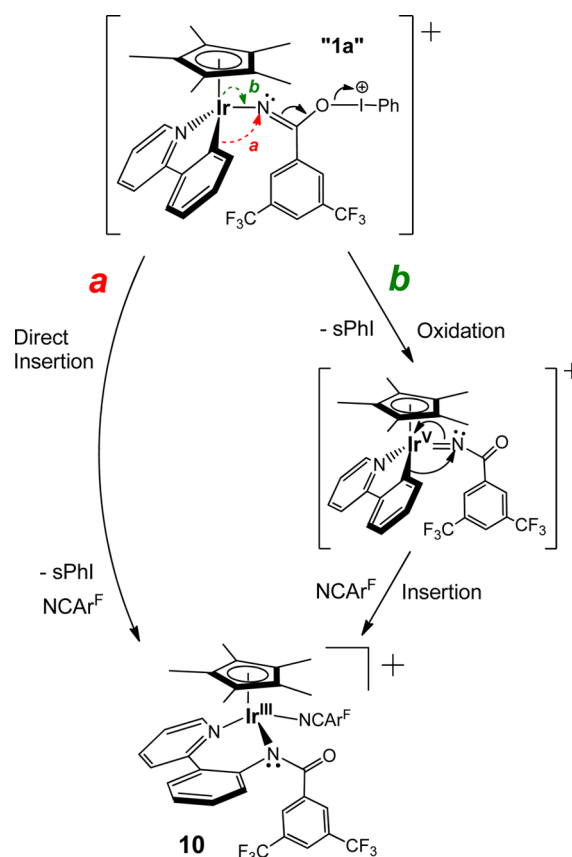
Scheme 12. Rate of OAT to **1 (Top) and Rate of NCAr^{F} Dissociation from **1** (Bottom)**



Since the rate of the first oxidation step was too fast to monitor under our conditions, ligand substitution experiments were conducted to measure the rate constant of nitrile dissociation from iridium. When 6 equiv of triphenylphosphine was added to **1**, first-order kinetics for the conversion of **1** to $[\text{Ir}(\text{Cp}^*)(\text{phpy})(\text{PPh}_3)]^+$ (**1-PPh₃**) were observed at $-40\text{ }^{\circ}\text{C}$. The first-order rate constant for conversion of **1** to **1-PPh₃** was determined to be $6.19 \times 10^{-4} \text{ s}^{-1}$ ($R^2 = 0.998$). In addition to PPh_3 , acetonitrile was also selected for ligand substitution. Although acetonitrile is not a strong ligand, full displacement of NCAr^{F} was observed, forming $[\text{Ir}(\text{Cp}^*)(\text{phpy})(\text{NCCH}_3)]^+$ (**1-NCCH₃**).^{39,61} When 30 equiv of acetonitrile was added to **1** at $-40\text{ }^{\circ}\text{C}$, first-order kinetics were also observed, and the rate of conversion to **1-NCCH₃** was determined to be $6.05 \times 10^{-4} \text{ s}^{-1}$ ($R^2 = 0.999$). Good agreement between the observed rates for conversion of **1** to the PPh_3 and acetonitrile adducts indicated that the values reflected the rate of NCAr^{F} dissociation from **1** ($\sim 6 \times 10^{-4} \text{ s}^{-1}$). Since the rate of oxidation is much faster than the rate of nitrile dissociation from **1**, direct oxidation of the coordinated nitrile must occur (sPhIO does not oxidize NCAr^{F} in the absence of iridium). Oxidation of a coordinated nitrile to an amide has been observed only rarely.^{62–64}

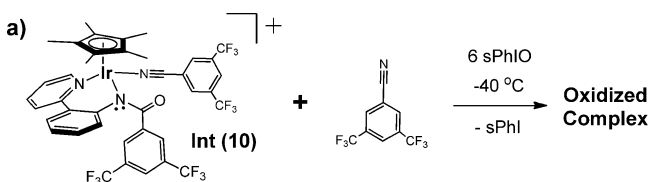
Oxidation is likely to occur via nucleophilic attack of sPhIO on the nitrile carbon of a σ -bound NCAr^{F} ligand,⁶⁵ akin to well-established hydrolysis mechanisms of coordinated nitriles.⁶⁶ Importantly, complex **1** does not react with water in solution at room temperature, which rules out product formation via nitrile hydrolysis. The oxidations here were run under anhydrous conditions. The reagent sPhIO is considered to be nucleophilic (the reported bond distance between the iodine and oxygen is characteristic of a single bond, which leaves extra electron density on the oxygen).⁶⁷ Initial attack of sPhIO at the central carbon of NCAr^{F} on **1** would yield the intermediate “**1a**” pictured at the top of Scheme 13. Migration of two electrons is

Scheme 13. Possible Mechanisms for Nitrile Oxidation and Insertion

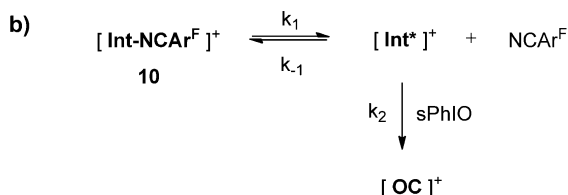


required to break the oxygen–iodine bond of sPhIO and release sPhI. These electrons could come (route a) directly from the iridium–carbon bond of phpy, which would accomplish insertion in a one-step concerted process without accessing the Ir(V) oxidation state. Alternatively, in a two-step process, the metal could be oxidized (route b), generating a transient Ir(V)nitrene ripe for insertion. A recently reported catalytic amidation reaction of arenes with cyclometalating directing groups using an Ir(Cp*)-based catalyst led to two possible analogous mechanisms (direct insertion versus metal oxidation and insertion).⁶⁸ The catalytic reaction employed acyl azides as the amide source, effectively a two-electron oxidant. In addition, a reported oxidation of an $[\text{Ir}(\text{Cp}^*)(\text{phpy})\text{NCCH}_3]^+$ complex with the nitrene transfer reagent PhINTs led to sulfonamide insertion into the iridium–carbon bond of phpy.⁶¹ An Ir^V–nitrene intermediate was postulated. Less than a dozen stable Ir(III) complexes with multiply bound nitrogen ligands are known, but stable Ir^V–nitrenes have not been reported.⁶⁹ From our experimental evidence, an Ir^V–nitrene is neither implicated nor excluded in the first oxidation step of **1** with sPhIO.

Mechanism of the Second Oxidation Step. The kinetics of oxidation from the intermediate **10** to the **OC** were studied in the presence of excess nitrile ligand. Plots of $\ln[\mathbf{10}]$ versus time showed linear behavior when the reactions were run in the presence of excess sPhIO. It was found that the rate of reaction was inhibited by excess nitrile (Scheme 14a). For example, the second-order rate constant for oxidation in the absence of added nitrile ligand was $[1.68(\pm 0.13)] \times 10^{-3} \text{ M}^{-1} \text{ s}^{-1}$, but when 45 equiv of nitrile was added, the rate slowed to

Scheme 14. (a) Kinetics of OAT to **10** in the Presence of NCAR^F and (b) Proposed Reaction Pathway

Equivalents Nitrile	Observed Rate Constant
0 equiv	$1.68 (\pm 0.13) \times 10^{-3} \text{ M}^{-1} \text{ s}^{-1}$
5 equiv	$1.38 (\pm 0.08) \times 10^{-3} \text{ M}^{-1} \text{ s}^{-1}$
15 equiv	$1.21 (\pm 0.06) \times 10^{-3} \text{ M}^{-1} \text{ s}^{-1}$
45 equiv	$0.65 (\pm 0.06) \times 10^{-3} \text{ M}^{-1} \text{ s}^{-1}$



$[0.65(\pm 0.06)] \times 10^{-3} \text{ M}^{-1} \text{ s}^{-1}$. Adding 5 or 15 equivalents of nitrile also slowed the rate of the reaction, but only marginally in comparison to the reaction with no added NCAR^F. Inhibition from added NCAR^F suggested that dissociation of NCAR^F was necessary for the second oxidation step to occur. Direct oxidation of the Cp* or the pppy ligand **8** was not implicated, as sPhIO and the neutral iridium-chloride complex **9** did not react at -40°C .

Postulated elementary steps for the second oxidation are depicted in Scheme 14b. The reaction was assumed to be first-order in the sPhIO reagent, although no attempt was made to determine the dependence of the rate constant on the sPhIO concentration. When the steady-state approximation is applied to **Int***, the five-coordinate iridium species resulting from dissociation of NCAR^F, the rate law shown in eq 1 can be

$$\text{rate} = \frac{k_1 k_2 [\mathbf{10}] [\text{sPhIO}]}{k_{-1} [\text{NCAR}^{\text{F}}] + k_2 [\text{sPhIO}]} \quad (1)$$

derived. The sPhIO concentration was treated as a constant in the oxidation reactions, since complete dissolution of a 6-fold molar excess of sPhIO (relative to **10**) was achieved. The observed rate constant (k_{obs}), therefore, was described in terms of the rate constants of the elementary steps and the concentration of sPhIO (eq 2). When the reciprocals of the

$$\text{rate} = k_{\text{obs}} [\mathbf{10}] \quad k_{\text{obs}} = \frac{k_1 k_2 [\text{sPhIO}]}{k_{-1} [\text{NCAR}^{\text{F}}] + k_2 [\text{sPhIO}]} \quad (2)$$

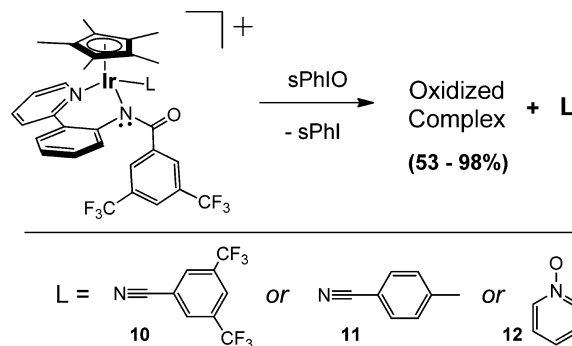
four k_{obs} values were plotted against their respective concentrations of the nitrile ligand (eq 3), the data points were fitted by linear regression and yielded an R^2 value of 0.988

$$1/k_{\text{obs}} = \left(\frac{k_{-1}}{k_1 k_2 [\text{sPhIO}]} \right) [\text{NCAR}^{\text{F}}] + \frac{1}{k_1} \quad (3)$$

(Supporting Information). The rate constant for dissociation of nitrile (k_1) from **10** was estimated to be $1.7 \times 10^{-3} \text{ s}^{-1}$, and the ratio k_2/k_{-1} was calculated from the slope of the regression to be ~ 4.5 . The rate of oxidation of **Int***, therefore, is roughly 5 times faster than trapping with NCAR^F. The kinetic data are consistent with reversible nitrile dissociation that competes with irreversible oxidation. Notably, dissociation of nitrile in the second oxidation step contrasted starkly with behavior observed in the first oxidation step, where coordinated NCAR^F underwent nucleophilic attack.

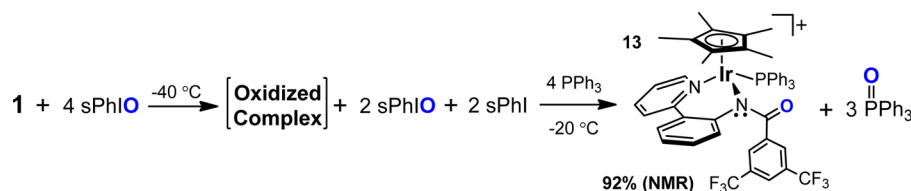
To ascertain whether or not NCAR^F was perhaps oxidized after OAT to the metal center, we prepared and oxidized analogues of the **Int** using the different trapping ligands *p*-tolunitrile (NCAR^{Me}) and pyridine *N*-oxide (OPy). Notably, OPy is resistant to oxidation. If oxidation of the various analogues yielded the **OC** in each case, it would suggest that the sixth ligand of the intermediate was inconsequential to the formation of the **OC**. Accordingly, the complexes $[\text{Ir}(\text{Cp}^*)\{3,5\text{-bis}(\text{trifluoromethyl})\text{benzoyl}\}(2\text{-}(2\text{-pyridyl})\text{phenyl})\text{amide}\}\text{-}(\text{NCAR}^{\text{Me}})][\text{B}(\text{Ar}^{\text{F}})_4]$ (**11**, **Int-NCAR^{Me}**) and $[\text{Ir}(\text{Cp}^*)\{3,5\text{-bis}(\text{trifluoromethyl})\text{benzoyl}\}(2\text{-}(2\text{-pyridyl})\text{phenyl})\text{amide}\}\text{-}(\text{OPy})][\text{B}(\text{Ar}^{\text{F}})_4]$ (**12**, **Int-OPy**) were prepared following the same strategy described for the synthesis of **10**.

Oxidation of both **Int-NCAR^{Me}** and **Int-OPy** with excess sPhIO yielded 1 equiv of sPhI and the same **OC** as **10** (Scheme 15).

Scheme 15. Formation of the **OC** using Different κ^1 Ligands

The oxidation of **Int-OPy** gave the **OC** in 98% yield (using an internal standard) after 25 min at -30°C . Apparently OPy binds more tightly to iridium than NCAR^F and required increased temperatures and more time for the reaction to reach completion. Higher temperatures yet (-20°C) were required to observe a reaction with **Int-NCAR^{Me}**, which is consistent with a dissociative mechanism and the use of NCAR^{Me}, a ligand more strongly binding than NCAR^F or OPy. After 45 min, the yield of the **OC** peaked at 53% and then began to decline (internal standard), even though full conversion of **Int-NCAR^{Me}** had not occurred. Presumably after 45 min, the rate of decomposition of the **OC** surpassed the rate of formation of the **OC** via reaction of **Int-NCAR^{Me}** and sPhIO. Decomposition products were observed in the ^1H NMR experiment, which was consistent with the appearance of decomposition products in the oxidation of **1** with sPhIO at -20°C . Importantly, free nitrile ligand or free OPy was observed in the ^1H NMR spectra after oxidation of **10**, **11**, or **12**.

Conversion of the cationic intermediate to the **OC** is thus independent of the identity of the κ^1 ligand. In addition, oxidation of **1** in the absence of excess NCAR^F also rapidly generated the **OC**, despite the fact that no nitrile was available after coordinated NCAR^F was oxidized in the first OAT step.

Scheme 16. Reaction of the OC with PPh₃

That the yield of the OC is higher with OPy as the sixth ligand (98%) of the intermediate than with NCAR^F as the sixth ligand (90%) may reflect the fact that OPy is stable to oxidation. These experiments, in addition to the observation of free nitrile or OPy in the ¹H NMR spectra, confirmed that the sixth ligands in **10**–**12** were not oxidized after dissociation and simply acted as placeholder ligands.

Oxidation of the intermediate **10**, therefore, requires NCAR^F dissociation from iridium and yields a species that does not react with free NCAR^F. Nitrile dissociation from intermediate **10** exposes an electrophilic Ir(III) center, which the nucleophilic sPhIO oxidant can attack.⁷⁰ Importantly, the OC is not simply a coordinated sPhIO molecule in the sixth coordination site, as 1 equiv of sPhI is generated, indicating complete transfer of the oxygen atom to iridium. Although the exact identity of the OC is not clear from the spectroscopic data, several possibilities are offered that reflect dissociation of the sixth ligand and incorporation of a second oxygen atom. These include, but are not limited to, an Ir^V-oxo complex, an Ir^{III}-iminopercarboxylate complex (with a fused 5,6-membered iridacycle and a coordinated peroxide), Ir(V) dimers with bis- μ -oxo ligands, and an Ir^{III}-hydroxamate complex (oxygen atom insertion into the iridium–nitrogen bond of the benzamide donor). Importantly, a mononuclear Ir^V-oxo complex might be expected to be paramagnetic like the known isoelectronic Ru^{IV}-oxo complexes, which would complicate observation by NMR spectroscopy.⁷¹ Terminal metal oxo ligands can also interact to form bis- μ -oxo dimers.⁷² An Ir^{III}-iminopercarboxylate complex could form via nucleophilic attack of the amide either on a terminal, electrophilic oxo ligand (reducing the metal to Ir(III) and forming an oxygen–oxygen bond) or on the oxygen atom of a coordinated sPhIO molecule. The amide served as a base in the presence of HCl; therefore, it might also serve as a nucleophile. Insertion into the iridium–nitrogen bond of the benzamide is a plausible pathway for hydroxamate formation.

The reactivity of the OC was explored to see if it could act as an oxidant. The OC did not react with styrene, *trans*-stilbene, or 2,3-dimethyl-2-butene at -20 °C. In addition, the OC did not react with water (delivered as a solution in acetone-*d*₆) between -40 and -20 °C. However, when 4 equiv of PPh₃ was added to a freshly generated solution of the OC and warmed to -20 °C, phosphine oxidation to the oxide (O=PPh₃) was observed, in addition to a new iridium species (92% conversion, internal standard) after 75 min (Scheme 16). The iridium complex was identified as [Ir(Cp*){(3,5-bis(trifluoromethyl)benzoyl)(2-(2-pyridyl)phenyl)amide}(PPh₃)₃][B(Ar^F)₄]⁺ (**13**) by comparing the ¹H NMR spectrum to the spectrum of an independently prepared sample of **13**. Notably, the Cp* methyl protons of the new iridium species and complex **13** resonated at 1.32 and 1.31 ppm, respectively. In addition, the aromatic regions in the ¹H NMR spectra were essentially identical (Supporting Information). Complex **13** has been fully characterized, and crystals suitable for X-ray diffraction studies

were grown by layering pentane on top of a concentrated solution of **13** in dichloromethane. The structure of **13** revealed the coordinated benzamide functionality with a C–N bond length of 1.357 Å and a C=O bond length of 1.228 Å (Figure 8). For

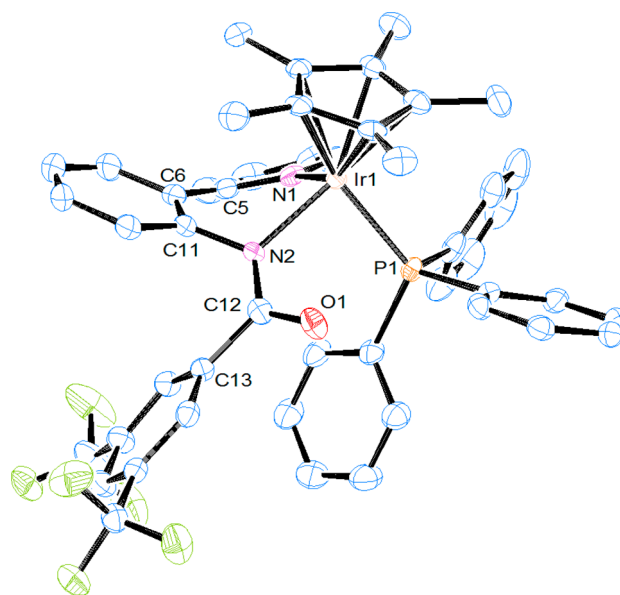


Figure 8. ORTEP drawing of **13**, with partial numbering scheme (50% probability thermal ellipsoids). The anion and all hydrogen atoms are omitted for clarity. Selected bond lengths (Å), bond angles (deg), and torsion angles (deg): Ir₁–P₁ 2.3594(6), Ir₁–N₁ 2.151(2), Ir₁–N₂ 2.105(2), N₂–C₁₂ 1.357(4), N₂–C₁₁ 1.420(3), O₁–C₁₂ 1.228(3); Ir₁–N₂–C₁₂ 122.93(17), C₁₁–N₂–C₁₂ 119.3(2), N₂–C₁₂–O₁ 123.4(2), N₂–C₁₂–C₁₃ 119.3(2); C₁₁–C₆–C₅–N₁ 35.3(4).

comparison, the iminol functionality of **7** included a C=N bond distance of 1.294 Å and a C–O bond distance of 1.316 Å, which are distinct from those of **13**.

The source of the oxygen atoms in the phosphine oxidation reaction was closely examined. Importantly, the calculated O=PPh₃/13 ratio was 3.0 at the end of the reaction, on the basis of integration of the ¹H NMR spectrum (Supporting Information). The sPhIO oxidant is known to react with phosphine in the absence of metal.⁴⁰ Only 2 equiv of the sPhIO reagent (out of 4 equiv) reacted with iridium starting material **1** to form the OC. Two equivalents of O=PPh₃, therefore, was ascribed to direct oxidation of PPh₃ by residual sPhIO. The third oxidative equivalent, however, could only be accounted for by OAT from the OC. This conclusion was strengthened by the fact that the third equivalent of O=PPh₃ grew in concomitantly with the appearance of **13**. This behavior is consistent with direct OAT from the OC to PPh₃. OAT from the OC leaves a vacant coordination site, which is trapped by PPh₃ to form **13**. Notably, the (mesityl)₃Ir^V-oxo complex has been reported to oxidize phosphines and arsines but does not react with olefins

or water.⁷ The oxidized complex, therefore, holds the capacity to cleanly oxidize PPh₃ and regenerate the same Cp*/κ² ligand framework of intermediate **10**. This serves as a unique example of an oxidized Ir(Cp*) complex that reacts to form a well-characterized, molecular product.

CONCLUSIONS

Oxidation of **1** with the OAT reagent sPhIO yielded a single, molecular compound at -40 °C. This is a rare example of an Ir(Cp*) complex related to water oxidation catalysts that has not suffered from Cp* ligand decomposition when oxidized. When the oxidized complex could not be isolated, ligands corresponding to potential oxidation of phpy by oxygen atom insertion into the iridium-carbon and/or iridium-nitrogen bonds were synthesized and metalated. Complex **4**, with a κ² ligand modeling insertion into the iridium carbon bond of phpy, formed an unreactive phenoxide-bridged iridium dimer (**6**) upon chloride abstraction. Another iridium complex (**5**), with a κ² ligand representing the product of oxygen atom insertion into the iridium-carbon and iridium-nitrogen bonds of phpy, was sensitive to moisture, and the bidentate ligand was cleaved from iridium. Two sequential OAT reactions were then uncovered in the low-temperature oxidation of **1**, and an intermediate was isolated and characterized. The intermediate revealed that OAT to the carbon of the nitrile ligand coupled with insertion into the iridium-carbon bond of phpy had occurred in the first step. Nucleophilic attack of the oxidant on the coordinated nitrile was implicated, and an Ir^V-nitrene may have been generated transiently. The second OAT was found to occur upon ligand dissociation from iridium, but the oxidized complex could not be identified. OAT from the oxidized complex to phosphine, however, was observed in high yield and regenerated an iridium complex with the same Cp* and benzamide ligands as the intermediate **10**. This work offers insights into possible deactivation pathways for iridium complexes under harsh oxidizing conditions and describes the reactivity and product identity of an oxidized, molecular iridium species.

EXPERIMENTAL SECTION

Materials and Methods. All reactions were performed under an atmosphere of dry argon using standard Schlenk and drybox techniques, unless noted otherwise. Argon was purified by passage through columns of BASF R3-11 catalyst and 4 Å molecular sieves. Methylene chloride, hexane, and pentane were purified under an argon atmosphere and passed through a column packed with activated alumina. All other chemicals were used as received without further purification. ¹H and ¹³C NMR spectra were recorded on Bruker AVANCEIII400, AVANCEIII500, and AVANCEIII600 spectrometers. ¹H NMR and ¹³C NMR chemical shifts were referenced to residual ¹H and ¹³C signals of the deuterated solvents. Unless stated otherwise, yields of NMR reactions were determined using hexamethyldisiloxane as an internal standard. IR absorption spectroscopy was carried out on a Bruker Alpha-P ATR absorption spectrophotometer. X-ray diffraction studies were conducted on a Bruker-AXS SMART APEX-II diffractometer. Crystals were selected and mounted using Paratone oil on a MiteGen Mylar tip. Elemental analyses were performed by Robertson Microlit Laboratories of Madison, NJ. **Caution!** An explosion hazard has been reported using the initially published procedure for preparation of the OAT reagent 2-*tert*-butylsulfonyl-iodosobenzene (sPhIO).^{40,41} In this work we have used a recent procedure published by Lin.⁴²

Kinetics. Ligand Dissociation. Complex **1** (8.0 mg, 5 μmol) was dissolved in dichloromethane-*d*₂ and added slowly to a chilled solution (-40 °C) of PPh₃ (7.4 mg, 28 μmol) or acetonitrile (8 μL, 150 μmol)

in dichloromethane-*d*₂. The total solution volume was 800 μL. The ligand displacement reaction was monitored by ¹H NMR spectroscopy at -40 °C, and the concentration of **1** was calculated from the ratio of the Cp* integrals for **1** and the respective adduct. Plotting ln [**1**] as a function of time yielded graphs displaying good linear behavior (Supporting Information).

Oxidation of **10 with sPhIO in the Presence of NCAR^F.** A 10 mg portion of sPhIO (29 μmol) was completely dissolved in dichloromethane-*d*₂ at room temperature and then chilled to -78 °C. The sPhIO remained in solution when cooled. A solution with 9.0 mg of dissolved **10** (5 μmol) and NCAR^F (0–45 equiv) in dichloromethane-*d*₂ was slowly added to the sPhIO solution at -78 °C, bringing the total sample volume to 800 μL. The oxidation reaction was monitored by ¹H NMR spectroscopy at -40 °C, and the concentration of **10** was calculated from the ratio of the Cp* integrals for **10** and the **OC**. Plotting ln [**10**] versus time yielded charts with good linear correlation (Supporting Information).

Synthesis of [Ir(Cp*)(phpy)NCAR^F][B(Ar^F)₄] (1**).** The synthetic procedure has been reported previously.³⁹

Synthesis of [Ir(Cp*)(phpy)NCAR^F][SbF₆] ([1**][SbF₆]).** In a 100 mL Schlenk flask, 150 mg of Ir(Cp*)(phpy)Cl (0.29 mmol), 52 μL of NCAR^F (0.31 mmol), 105 mg of AgSbF₆ (0.31 mmol), and 20 mL of dichloromethane were combined. The mixture was stirred for 4 h in the dark, at which point the mixture was filtered by cannula. The solvent was reduced to a minimal volume and added slowly to rapidly stirred pentane chilled to -78 °C. The solid was isolated by filtration and dried by heating to 40 °C overnight under high vacuum, yielding 206 mg of the product (74%). ¹H NMR (500 MHz, CD₂Cl₂): δ 8.80 (d, *J* = 6.0, 1H), 8.12 (s, 1H), 7.95 (m, 2H), 7.92 (s, 2H), 7.80 (d, *J* = 7.5, 1H), 7.78 (d, *J* = 7.5, 1H), 7.37 (t, *J* = 6.5, 1H), 7.32 (t, *J* = 6.5, 1H), 7.23 (t, *J* = 7.5, 1H), 1.75 (s, 15H).

Synthesis of the "Oxidized Complex" (OC**).** A solution of 10 mg of **1** (6 μmol) in 0.4 mL of dichloromethane-*d*₂ was slowly added to an NMR tube charged with 8 mg of sPhIO (24 μmol, 4 equiv) and cooled to -40 °C. The mixture was thoroughly mixed for 1 min using a thin copper wire. The sample was transported cold (-78 °C) to an NMR probe cooled to -40 °C. ¹H NMR spectroscopy revealed 91% conversion of **1** to the **OC**. Alternatively, a solution of 7 mg of **10** (4 μmol) in 0.4 mL of dichloromethane-*d*₂ was slowly added to an NMR tube charged with 7 mg of sPhIO (21 μmol, 5 equiv) and cooled to -40 °C. The mixture was thoroughly mixed for 4 min using a thin copper wire. Conversion to the **OC** (90%) was confirmed by ¹H NMR spectroscopy at -40 °C (using the 4-proton resonance of the [B(Ar^F)₄] anion at 7.54 ppm as an internal standard). The **OC** was unstable above -20 °C. ¹H NMR (500 MHz, CD₂Cl₂, -40 °C, multiple resonances were obscured): δ 8.80 (d, *J* = 5.0, 1H), 7.89 (d, *J* = 7.5, 1H), 7.78 (s, 1–2H), 7.71 (s, 8H), 7.60 (m, 1–2H), 7.53 (s, 4H), 7.10 (m, 2H), 6.47 (m, 1H), 1.21 (s, 15H). ¹³C{¹H} NMR (125 MHz, CD₂Cl₂, -40 °C, one carbon was not observed): δ 171.1, 161.5 (1:1:1:1 quartet, *J*_{C-B} = 49), 154.5, 152.4, 145.0, 140.2, 139.6, 136.1, 134.5, 133.6, 131.5, 130.5, 129.7, 128.5 (q, 2-bond *J*_{C-F} = 32), 127.7, 125.7, 124.9, 124.3 (q, 1-bond *J*_{C-F} = 270), 123.9, 122.8 (q, 1-bond *J*_{C-F} = 271), 117.3, 86.2, 8.6.

Synthesis of 2-(2-Hydroxyphenyl)pyridine (2**).** In a thick-walled, 100 mL glass vessel, 333 mg of 2-(2-hydroxyphenyl)pyridine *N*-oxide (1.8 mmol), 1.06 g of ammonium formate (16.8 mmol, 9.5 equiv), 80 mg of 5% Pd/C (2 mol %), and 16 mL of methanol were added. The reaction vessel was sealed, covered with aluminum foil, and heated to 95 °C overnight. After it was cooled to room temperature the next morning, the mixture was filtered and the solvent was removed under reduced pressure. The oil was diluted with dichloromethane and eluted through a silica gel column with dichloromethane/hexane mixtures. After the solvent was removed under reduced pressure, 183 mg of a pale yellow oil was isolated (60%). The product matched the spectral properties previously reported⁴⁵ for this compound. ¹H NMR (500 MHz, CD₂Cl₂): δ 14.27 (s, O-H, 1H), 8.52 (d, *J* = 4.5, 1H), 7.95 (d, *J* = 8.5, 1H), 7.88 (t, *J* = 7.5, 1H), 7.83 (d, *J* = 8.0, 1H), 7.29 (m, 2H), 6.96 (d, *J* = 8.5, 1H), 6.91 (t, *J* = 7.0, 1H).

Synthesis of 2-(2-Hydroxyphenyl)pyridine *N*-Oxide (3**).** In a glovebox, 118 mg of Pd(OAc)₂ (0.53 mmol, 5 mol %), 460 mg of

[HP^tBu₃]BF₄ (1.58 mmol, 14 mol %), 2.9 g of K₂CO₃ (21 mmol, 1.9 equiv), and 4 g of pyridine *N*-oxide (42 mmol, 3.8 equiv) were placed in a 100 mL pressure flask. Toluene (20 mL) was added, followed by 1.3 mL of 2-bromophenol (11 mmol, 1 equiv). The reaction vessel was closed securely, brought out of the glovebox, and heated to 135 °C overnight with stirring. The next morning, the mixture was cooled to room temperature and filtered through Celite. The Celite was washed twice with dichloromethane and then twice with acetone. The solvent was removed, and the crude material was chromatographed on silica gel using acetone/hexane (1/4 v/v, R_f = 0.07). The product fractions were collected, the solvent was removed, and the solid was heated to 50 °C under vacuum overnight. A 940 mg amount of product was isolated (45%). Anal. Calcd (found) for C₁₁H₉NO₂: C, 70.58 (70.33); H, 4.85 (4.80); N, 7.48 (7.38). ¹H NMR (400 MHz, CD₂Cl₂): δ 11.16 (s, 1H), 8.40 (d, *J* = 6.5, 1H), 7.69 (d, *J* = 8.5, 1H), 7.59 (t, *J* = 7.5, 1H), 7.46 (t, *J* = 8.0, 1H), 7.42 (m, 2H), 7.03 (m, 2H). ¹³C{¹H} NMR (150 MHz, CD₂Cl₂): δ 159.7, 151.4, 140.5, 132.5, 131.4, 130.0, 129.3, 124.7, 121.4, 120.4, 120.3.

Synthesis of Ir(Cp*)(2-(2-pyridyl)phenoxy)Cl (4). A Schlenk flask was charged with 92 mg of NaH (3.8 mmol), 35 mL of THF, and 92 μL of 2-(2-hydroxyphenyl)pyridine (109 mg, 0.63 mmol). The mixture was stirred at room temperature for 45 min and then filtered by cannula onto a sample of 225 mg of [Ir(Cp*)(Cl)₂]₂ (0.28 mmol) that had previously been heated to 50 °C under vacuum for 18 h. The mixture was stirred for 7 h and then filtered. The solvent was reduced to a minimal volume under reduced pressure and then was added slowly to rapidly stirred pentane (20 mL) chilled to -78 °C. The solid was collected by filtration and then eluted through a silica gel column using acetone/dichloromethane (1/4 v/v). The solvent was removed under reduced pressure, and the yellow solid was heated to 50 °C under high vacuum overnight, yielding 230 mg of product (76%). Yellow crystals suitable for X-ray diffraction analysis were grown by vapor diffusion of pentane into a concentrated solution of the product in dichloromethane. Using Olex2,^{73a} the structure was solved with the olex2.solve structure solution program using charge flipping and refined with the XL refinement package using least-squares minimization.^{73b} Crystal data for C₂₁H₂₃NOClIr (M_r = 533.05): monoclinic, space group P2₁/c (No. 14), *a* = 7.22210(10) Å, *b* = 14.9351(2) Å, *c* = 17.0443(2) Å, β = 93.7670(10)°, *V* = 1834.47(4) Å³, *Z* = 4, *T* = 100 K, μ(Cu Kα) = 15.486 mm⁻¹, *D*_{calcd} = 1.930 g/mm³, 33119 reflections measured (7.88 ≤ 2θ ≤ 140.5), 3490 unique (R_{int} = 0.0319), which were used in all calculations. The final R1 value was 0.0207 (>2σ(*I*)), and the wR2 value was 0.0472 (all data), with a goodness of fit on *F*² of 1.181. Anal. Calcd (found) for C₂₁H₂₃ClIrNO: C, 47.31 (47.10); H, 4.35 (4.34); N, 2.63 (2.46). ¹H NMR (500 MHz, CD₂Cl₂): δ 8.72 (d, *J* = 5.5, 1H), 7.78 (t, *J* = 8.0, 1H), 7.72 (d, *J* = 8.0, 1H), 7.49 (d, *J* = 7.5, 1H), 7.21 (overlapping triplets, *J* = 7.0 and 7.5, 2H), 6.91 (d, *J* = 8.0, 1H), 6.63 (t, *J* = 7.5, 1H), 1.34 (s, 15H). ¹³C{¹H} NMR (100 MHz, CD₂Cl₂): δ 169.2, 155.7, 153.8, 138.2, 131.4, 128.8, 128.2, 123.1, 122.9, 122.2, 116.5, 84.6, 8.6.

Synthesis of Ir(Cp*)(2-(2-pyridyl)phenoxy *N*-oxide)Cl (5). In a 100 mL Schlenk flask, 93 mg of 2-(2-hydroxyphenyl)pyridine *N*-oxide (0.5 mmol), 100 mg of NaH (4.2 mmol), and 70 mL of THF were added. The mixture was stirred at room temperature overnight. Simultaneously, 187 mg of [Ir(Cp*)(Cl)₂]₂ (0.24 mmol) was heated at 50 °C under high vacuum overnight. The next day, the THF solution was filtered with a cannula onto the metal dimer. The mixture was stirred for 1.5 h at room temperature, after which time the mixture was filtered by cannula. The solvent was removed from the filtrate, and the resulting solid was redissolved in minimal dichloromethane. The solution was slowly added to rapidly stirred pentane chilled to -78 °C. The supernatant was filtered off by cannula, and 135 mg of a red solid was isolated after drying under high vacuum overnight (52%). The compound was stored in a glovebox freezer. Orange crystals suitable for X-ray diffraction were grown by storing a saturated solution of the product in pentane at -25 °C. Using Olex2,^{73a} the structure was solved with the olex2.solve structure solution program using charge flipping and refined with the XL refinement package using least-squares minimization.^{73b} Crystal data for C₂₃H₂₇Cl₃IrNO₂ (M_r = 718.91): triclinic, space group P $\bar{1}$ (No. 2), *a* = 9.1491(4) Å, *b* = 10.4209(4) Å,

c = 14.3917(6) Å, α = 75.867(2)°, β = 87.839(2)°, γ = 74.111(2)°, *V* = 1279.14(9) Å³, *Z* = 2, *T* = 100 K, μ(Cu Kα) = 15.083 mm⁻¹, *D*_{calcd} = 1.867 g/mm³, 23060 reflections measured (6.34 ≤ 2θ ≤ 140.34), 4711 unique (R_{int} = 0.0304), which were used in all calculations. The final R1 value was 0.0216 (>2σ(*I*)), and the wR2 value was 0.0529 (all data), with a goodness of fit on *F*² of 1.086. Anal. Calcd (found) for C₂₁H₂₃ClIrNO₂: C, 45.94 (47.14); H, 4.22 (4.50); N, 2.55 (2.27). ¹H NMR (500 MHz, CD₂Cl₂): δ 8.17 (d, *J* = 6.0, 1H), 7.73 (t, *J* = 7.5, 1H), 7.36 (d, *J* = 8.0, 1H), 7.33 (td, *J* = 7.0 and 1.5, 1H), 7.28 (td, *J* = 7.5 and 1.5, 1H), 7.07 (dd, *J* = 7.5 and 1.5, 1H), 6.93 (d, *J* = 7.5, 1H), 6.65 (t, *J* = 7.0, 1H), 1.55 (s, 15H). ¹³C{¹H} NMR (150 MHz, CD₂Cl₂): δ 166.5, 155.9, 143.9, 134.4, 131.6, 131.1, 128.8, 127.4, 124.8, 121.7, 115.8, 81.7, 9.1.

Synthesis of [Ir(Cp*)(2-(2-pyridyl)-μ-phenoxy)]₂[B(Ar^F)₄]₂ (6). A 100 mL Schlenk flask was charged with 100 mg of Ir(Cp*)(2-(2-pyridyl)phenoxy)Cl (0.19 mmol), 207 mg of Na[B(Ar^F)₄] (0.23 mmol), and 30 mL of dichloromethane. After it was stirred for 7 h, the mixture was filtered and the solvent of the filtrate was removed. The solid was redissolved in a minimal volume of acetone and was slowly added to rapidly stirred pentane (20 mL) chilled to -78 °C. The mixture was filtered and the solid was heated to 40 °C overnight under vacuum, yielding 176 mg of a yellow solid (69%). Yellow crystals suitable for X-ray diffraction were grown by vapor diffusion of pentane into a concentrated solution of the product in dichloromethane. Using Olex2,^{73a} the structure was solved with the olex2.solve structure solution program using charge flipping and refined with the XL refinement package using least-squares minimization.^{73b} Crystal data for C₅₄H₃₇BCl₂F₂₄Ir₂NO (M_r = 1445.76): triclinic, space group P $\bar{1}$ (No. 2), *a* = 12.8140(2) Å, *b* = 13.7210(2) Å, *c* = 18.1145(3) Å, α = 106.1770(10)°, β = 110.3230(10)°, γ = 98.0160(10)°, *V* = 2767.97(7) Å³, *Z* = 2, *T* = 100.15 K, μ(Cu Kα) = 6.664 mm⁻¹, *D*_{calcd} = 1.735 g/mm³, 39637 reflections measured (5.56 ≤ 2θ ≤ 140.22), 10164 unique (R_{int} = 0.0210), which were used in all calculations. The final R1 value was 0.0237 (>2σ(*I*)) and the wR2 value was 0.0599 (all data), with a goodness of fit on *F*² of 1.087. Anal. Calcd (found) for C₁₀₆H₇₀N₂B₂F₄₈Ir₂O₂: C, 46.78 (46.91); H, 2.59 (2.54); N, 1.03 (1.08). ¹H NMR (500 MHz, CD₂Cl₂): δ 8.97 (d, *J* = 6.0, 2H), 8.23 (m, 4H), 7.89 (d, *J* = 8.0, 2H), 7.82 (m, 2H), 7.72 (s, 16H), 7.61 (t, *J* = 7.5, 2H), 7.55 (s, 8H), 7.28 (t, *J* = 7.5, 2H), 7.17 (d, *J* = 8.0, 2H), 0.59 (s, 30H). ¹³C{¹H} NMR (150 MHz, CD₂Cl₂): δ 162.1 (1:1:1:1 quartet, *J*_{C-F} = 50), 160.8, 154.3, 152.1, 141.9, 135.1, 133.9, 130.2, 129.2 (q, 2-bond *J*_{C-F} = 31), 127.7, 126.4, 125.9, 125.7, 124.9 (q, 1-bond *J*_{C-F} = 271), 122.1, 117.8, 85.9, 7.9.

Synthesis of [Ir(Cp*)(3,5-bis(trifluoromethyl)-*N*-(2-(2-pyridyl)phenyl)benziminol)Cl][B(Ar^F)₄] (7). A solution of 50 mg of **1** (0.032 mmol) in 1 mL of dichloromethane was added to an NMR tube chilled to -40 °C and charged with 40 mg of sPhIO (0.12 mmol). The reaction was mixed thoroughly for 1 min using a thin piece of copper wire, forming the OC. HCl(g) was then gently bubbled through the reaction for 1 min at -40 °C. The solids were allowed to settle, and the solution was decanted into an acetylation vial at room temperature. The organic layer was washed three times with water, and then the solvent was removed. The solids were washed three times with pentane and then recrystallized twice by layering pentane on top of a concentrated solution of **7** in dichloromethane. The solvents were decanted off, and the crystalline material was dried under high vacuum, yielding 16 mg of **7** (31%). Alternatively, **9** (56 mg, 0.072 mmol) was treated with HBF₄·OEt₂ (10 μL, 0.073 mmol) and stirred for 30 min in dichloromethane. A 68 mg portion of Na[B(Ar^F)₄] (0.077 mmol) was added, and the mixture was stirred for an additional 30 min before being filtered. The solvent was reduced to minimal volume, and the product was recrystallized by slowly adding the solution to rapidly stirred pentane chilled to -78 °C. The product was collected by filtration and dried under vacuum (93 mg, 79%). Yellow crystals suitable for X-ray diffraction were obtained by layering pentane on top of a concentrated solution of **7** in dichloromethane. Using Olex2,^{73a} the structure was solved with the olex2.solve structure solution program using charge flipping and refined with the XL refinement package using least-squares minimization.^{73b} Crystal data for C₆₂H₃₉BClF₃₀IrN₂O (M_r = 1636.41): monoclinic, space group P2₁/n (No. 14), *a* = 13.1858(3) Å, *b* = 20.1500(5) Å, *c* = 24.1403(6) Å, β = 100.1810(10)°, *V* = 6312.9(3) Å³,

$Z = 4$, $T = 100$ K, $\mu(\text{Cu } K\alpha) = 5.694 \text{ mm}^{-1}$, $D_{\text{calcd}} = 1.722 \text{ g/cm}^3$, 64683 reflections measured ($3.72 \leq 2\theta \leq 140.22$), 11930 unique ($R_{\text{int}} = 0.0407$), which were used in all calculations. The final $R1$ value was 0.0283 ($I > 2\sigma(I)$), the and $wR2$ value was 0.0695 (all data), with a goodness of fit on F^2 of 1.036. Anal. Calcd (found) for $\text{C}_{62}\text{H}_{39}\text{N}_2\text{BF}_3\text{IrOCl}$: C, 45.51 (45.21); H, 2.40 (2.20); N, 1.71 (1.71). ^1H NMR (600 MHz, CD_2Cl_2): δ 12.06 (s, 1H), 8.80 (d, $J = 6.0$, 1H), 8.12 (d, $J = 4.2$, 2H), 7.97 (s, 1H), 7.85 (dd, $J = 7.8$ and 1.8, 1H), 7.72 (s, 8H), 7.60 (overlapping triplets, $J \approx 5$, 2H), 7.56 (s, 4H), 7.56 (overlapping d, 1H), 7.40 (td, $J = 7.8$ and 1.2, 1H), 7.33 (td, $J = 7.8$ and 1.2, 1H), 6.57 (dd, $J = 7.8$ and 0.6, 1H), 1.33 (s, 15H). $^{13}\text{C}\{^1\text{H}\}$ NMR (150 MHz, CD_2Cl_2): δ 171.0, 162.1 (1:1:1:1 quartet, $J_{\text{C-B}} = 50$), 154.9, 154.4, 142.9, 141.7, 135.1, 132.8, 132.6 (q, 2-bond $J_{\text{C-F}} = 35$), 132.0, 131.8, 131.7, 130.0, 129.4, 129.2 (q, 2-bond $J_{\text{C-F}} = 32$), 127.0, 126.3 (pseudo t, 3-bond $J_{\text{C-F}} = 3$), 125.1, 125.0 (q, 1-bond $J_{\text{C-F}} = 272$), 124.9, 122.6 (q, 1-bond $J_{\text{C-F}} = 272$), 117.8 (pseudo t, 3-bond $J_{\text{C-F}} = 4$), 90.2, 8.4.

Synthesis of 3,5-Bis(trifluoromethyl)-N-(2-(2-pyridyl)phenyl)benzamide (8). A 2 dram acetylation vial was charged with 200 mg of 2-(2-pyridyl)aniline (1.18 mmol), 124 mg of NEt_3 (1.23 mmol), and 4 mL of dry dichloromethane and capped with a septum. After it was stirred for 10 min, the reaction mixture was stirred for an additional 10 min as the solution was cooled to 0°C . A 321 mg aliquot of 3,5-bis(trifluoromethyl)benzoyl chloride (1.16 mmol) was injected via syringe, and the reaction mixture was stirred overnight as the ice bath melted. The next day, 10 mL of dichloromethane was added, and the solution was washed once with water and twice with 1 M aqueous NaOH. The organic layer was dried with MgSO_4 and filtered, and the solvent was removed under reduced pressure. The crude product was chromatographed on silica gel using ethyl acetate/hexane (15/85 v/v, $R_f = 0.28$), and 414 mg of a white solid was isolated (87%). Anal. Calcd (found) for $\text{C}_{20}\text{H}_{12}\text{N}_2\text{F}_6\text{O}$: C, 58.54 (58.80); H, 2.95 (3.02); N, 6.83 (6.72). ^1H NMR (500 MHz, CD_2Cl_2): δ 14.01 (s, N-H, 1H), 8.80 (d, $J = 8.0$, 1H), 8.69 (d, $J = 5.0$, 1H), 8.56 (s, 2H), 8.09 (s, 1H), 7.93 (m, 2H), 7.86 (dd, $J = 8.0$ and 1.0, 1H), 7.51 (td, $J = 7.5$ and 1.0, 1H), 7.38 (td, $J = 5.0$ and 3.0, 1H), 7.28 (t, $J = 7.5$, 1H). $^{13}\text{C}\{^1\text{H}\}$ NMR (150 MHz, CD_2Cl_2): δ 162.3, 158.2, 147.4, 138.6, 138.2, 132.3 (q, 2-bond $J_{\text{C-F}} = 33$), 130.7, 129.1, 128.2, 128.1, 125.3, 125.2, 124.5, 123.6 (q, 1-bond $J_{\text{C-F}} = 271$), 123.3, 122.8, 121.8.

Synthesis of $[\text{Ir}(\text{Cp}^*)\{3,5\text{-bis(trifluoromethyl)benzoyl}\}(2\text{-pyridyl)phenyl)amide](\text{Cl})_2$ (9). A mixture of 150 mg of NaH (6.25 mmol), 450 mg of proligand 8 (1.10 mmol), and 30 mL of THF were stirred for 1.5 h and then filtered by cannula onto 400 mg of $[\text{Ir}(\text{Cp}^*)(\text{Cl})_2]_2$ (0.50 mmol). The iridium dimer had been dried by heating at 50°C under high vacuum the previous night. After the mixture was stirred for 24 h, the mixture was filtered by cannula and the solvent was removed under reduced pressure. The solid was redissolved in minimal dichloromethane and loaded onto a short (10 cm) silica gel column. Residual ligand was eluted first with dichloromethane, and then the metal species was eluted with acetone/dichloromethane mixtures (1/3 v/v, then 1/2 v/v). It was necessary to include NEt_3 (1%) in the eluent, since the metal species was basic and spread extensively as it traveled down the silica column. The product fractions were selected by their yellow solution color, and the solvent was removed. The solids were placed under high vacuum for 1.5 h, and 515 mg of a yellow solid was isolated (66%). Anal. Calcd (found) for $\text{C}_{30}\text{H}_{26}\text{N}_2\text{F}_6\text{IrOCl}$: C, 46.66 (46.80); H, 3.39 (3.38); N, 3.63 (3.69). ^1H NMR (400 MHz, CD_2Cl_2): δ 8.95 (d, $J = 6.0$, 1H), 7.92 (m, 2H), 7.81 (s, 2H), 7.67 (s, 1H), 7.56 (dd, $J = 8.0$ and 1.6, 1H), 7.34 (td, $J = 6.0$ and 3.2, 1H), 7.05 (td, $J = 7.6$ and 1.2, 1H), 6.93 (td, $J = 7.6$ and 1.2, 1H), 6.51 (d, $J = 8.0$, 1H), 1.41 (s, 15H). $^{13}\text{C}\{^1\text{H}\}$ NMR (150 MHz, CD_2Cl_2): δ 170.8, 156.0, 155.6, 150.4, 142.7, 139.1, 131.7, 130.7, 130.6 (q, 2-bond $J_{\text{C-F}} = 33$), 130.4, 130.3, 128.6, 124.4, 123.7 (q, 1-bond $J_{\text{C-F}} = 271$), 122.6, 122.5 (pseudo t, 3-bond $J_{\text{C-F}} = 4$), 122.4, 86.5, 8.7.

Synthesis of $[\text{Ir}(\text{Cp}^*)\{3,5\text{-bis(trifluoromethyl)benzoyl}\}(2\text{-pyridyl)phenyl)amide](\text{NCAr}^{\text{Me}})[\text{B}(\text{Ar}^{\text{F}})_4]$ (Int, 10). Complex 9 (150 mg, 0.19 mmol), 184 mg of $\text{Na}[\text{B}(\text{Ar}^{\text{F}})_4]$ (0.21 mmol), NCAr^{F} (3,5-bis(trifluoromethyl)benzotrile, 35 μL , 0.21 mmol), and 20 mL of dichloromethane were stirred for 3 h, at which point the mixture

was filtered by cannula. The solvent was reduced to a minimal volume, and the concentrated solution was added slowly to chilled, rapidly stirred pentane (20 mL). The solid was isolated by cannula filtration and then heated to 30°C under high vacuum for 3 days, yielding 283 mg of a yellow powder (79%). Anal. Calcd (found) for $\text{C}_{71}\text{H}_{41}\text{N}_3\text{BF}_3\text{IrO}$: C, 46.37 (46.53); H, 2.25 (2.22); N, 2.28 (2.20). ^1H NMR (600 MHz, CD_2Cl_2 , 5°C): δ 8.70 (d, $J = 6.0$, 1H), 8.20 (s, 2H), 8.15 (s, 1H), 8.11 (d, $J = 7.8$, 1H), 8.05 (t, $J = 7.8$, 1H), 7.76 (s, 3H), 7.72 (s, 8H), 7.63 (d, $J = 7.2$, 1H), 7.54 (s, 4H), 7.45 (t, $J = 6.6$, 1H), 7.15 (t, $J = 7.2$, 1H), 7.09 (t, $J = 7.2$, 1H), 6.55 (d, $J = 7.8$, 1H), 1.48 (s, 15H). $^{13}\text{C}\{^1\text{H}\}$ NMR (150 MHz, CD_2Cl_2 , 5°C , one carbon merged to others): δ 169.8, 162.9 (1:1:1:1 quartet, $J_{\text{C-B}} = 50$), 156.1, 153.9, 147.1, 141.2, 139.7, 135.0, 134.2, 133.4 (q, 2-bond $J_{\text{C-F}} = 35$), 131.5, 131.1, 131.0 (q, 2-bond $J_{\text{C-F}} = 33$), 130.5, 130.4, 129.0 (q, 2-bond $J_{\text{C-F}} = 29$), 128.5, 126.3, 124.8 (q, 1-bond $J_{\text{C-F}} = 272$), 125.2, 124.7, 123.5 (pseudo t, 3-bond $J_{\text{C-F}} = 4$), 123.2 (q, 1-bond $J_{\text{C-F}} = 272$), 122.0 (q, 1-bond $J_{\text{C-F}} = 272$), 117.9, 117.7 (pseudo t, 3-bond $J_{\text{C-F}} = 4$), 112.1, 90.8, 8.6.

Synthesis of $[\text{Ir}(\text{Cp}^*)\{3,5\text{-bis(trifluoromethyl)benzoyl}\}(2\text{-pyridyl)phenyl)amide](\text{NCAr}^{\text{Me}})[\text{B}(\text{Ar}^{\text{F}})_4]$ (Int-NCAr^{Me}, 11). Complex 9 (100 mg, 0.13 mmol), 127 mg of $\text{Na}[\text{B}(\text{Ar}^{\text{F}})_4]$ (0.14 mmol), NCAr^{Me} (*p*-tolunitrile, 17 μL , 0.14 mmol), and 20 mL of dichloromethane were stirred for 2 h, at which point the mixture was filtered by cannula. The solvent was reduced to a minimal volume, and the concentrated solution was added slowly to chilled, rapidly stirred pentane (20 mL). The solid was isolated by cannula filtration and then heated to 40°C under high vacuum overnight, yielding 148 mg of the product (67%). When 10 mg of 11 (0.006 mmol) and 14 mg of sPhIO (0.041 mmol) were mixed at -20°C in dichloromethane- d_2 , the OC was observed in 53% yield after 45 min by ^1H NMR spectroscopy. Anal. Calcd (found) for $\text{C}_{70}\text{H}_{43}\text{N}_3\text{BF}_3\text{IrO}$: C, 48.96 (48.69); H, 2.64 (2.63); N, 2.45 (2.28). ^1H NMR (500 MHz, CD_2Cl_2): δ 8.72 (dd, $J = 5.5$ and 0.5, 1H), 8.11 (d, $J = 7.5$, 1H), 8.06 (td, $J = 7.5$ and 1.5, 1H), 7.75 (s, 3H), 7.73 (s, 8H), 7.62 (dd, $J = 6.0$ and 1.5, 1H), 7.56 (s, 4H), 7.53 (d, $J = 8.0$, 2H), 7.46 (td, $J = 7.0$ and 1.5, 1H), 7.27 (d, $J = 8.0$, 2H), 7.12 (td, $J = 8.0$ and 1.5, 1H), 7.06 (td, $J = 7.5$ and 1.5, 1H), 6.50 (dd, $J = 7.5$ and 1.0, 1H), 2.38 (s, 3H), 1.49 (s, 15H). $^{13}\text{C}\{^1\text{H}\}$ NMR (150 MHz, CD_2Cl_2): δ 170.2, 162.1 (1:1:1:1 quartet, $J_{\text{C-B}} = 50$), 156.4, 153.9, 147.8, 147.6, 141.1, 140.7, 135.2, 133.6, 131.3, 131.2 (q, 2-bond $J_{\text{C-F}} = 33$), 131.1, 130.9, 130.7, 130.3, 129.3 (q, 2-bond $J_{\text{C-F}} = 31$), 128.7, 126.1, 125.0, 124.9 (q, 1-bond $J_{\text{C-F}} = 270$), 124.4, 123.4 (q, 1-bond $J_{\text{C-F}} = 272$), 123.3 (pseudo t, 3-bond $J_{\text{C-F}} = 4$), 121.6, 117.8 (pseudo t, 3-bond $J_{\text{C-F}} = 4$), 106.0, 90.3, 22.2, 8.7.

Synthesis of $[\text{Ir}(\text{Cp}^*)\{3,5\text{-bis(trifluoromethyl)benzoyl}\}(2\text{-pyridyl)phenyl)amide](\text{OPy})[\text{B}(\text{Ar}^{\text{F}})_4]$ (Int-OPy, 12). Complex 9 (90 mg, 0.12 mmol), 114 mg of $\text{Na}[\text{B}(\text{Ar}^{\text{F}})_4]$ (0.13 mmol), OPy (pyridine *N*-oxide, 0.13 mmol), and 20 mL of dichloromethane were stirred for 2 h, at which point the mixture was filtered by cannula. The solvent was reduced to a minimal volume and the concentrated solution was added slowly to chilled, rapidly stirred pentane (20 mL). The solid was isolated by cannula filtration and then dried under high vacuum overnight, yielding 150 mg of the red product (76%). Complex 12 was unstable in solution at room temperature after several hours. When 10 mg of 12 (0.006 mmol) and 18 mg of sPhIO (0.053 mmol) were mixed at -30°C in dichloromethane- d_2 , the OC was observed in 98% yield after 25 min by ^1H NMR spectroscopy. Anal. Calcd (found) for $\text{C}_{67}\text{H}_{43}\text{N}_3\text{BF}_3\text{IrO}_2$: C, 47.47 (47.18); H, 2.56 (2.49); N, 2.48 (2.29). ^1H NMR (500 MHz, CD_2Cl_2 , -40°C): δ 8.90 (d, $J = 5.0$, 1H), 8.07 (d, $J = 7.5$, 1H), 8.03 (t, $J = 7.5$, 1H), 7.74-7.70 (m, 5H), 7.71 (s, 8H), 7.54-7.52 (m, 2H), 7.53 (s, 4H), 7.34 (t, $J = 7.5$, 1H), 7.11 (t, $J = 7.0$, 2H), 6.99 (t, $J = 7.0$, 1H), 6.94 (t, $J = 7.5$, 1H), 6.32 (d, $J = 7.5$, 1H), 1.26 (s, 15H). $^{13}\text{C}\{^1\text{H}\}$ NMR (125 MHz, CD_2Cl_2 , -40°C , one carbon merged to others): δ 169.4, 161.6 (1:1:1:1 quartet, $J_{\text{C-B}} = 50$), 155.2, 153.5, 146.6, 141.6, 140.4, 139.6, 138.3, 135.2, 134.5, 130.8, 130.6, 129.6, 129.3, 128.6 (q, 2-bond $J_{\text{C-F}} = 31$), 125.9, 125.5, 124.3 (q, 1-bond $J_{\text{C-F}} = 271$), 123.9, 123.5, 122.9, 122.8 (q, 1-bond $J_{\text{C-F}} = 271$), 117.4, 86.2, 8.3.

Synthesis of $[\text{Ir}(\text{Cp}^*)\{3,5\text{-bis(trifluoromethyl)benzoyl}\}(2\text{-pyridyl)phenyl)amide](\text{PPh}_3)[\text{B}(\text{Ar}^{\text{F}})_4]$ (13). Complex 9 (57 mg, 0.074 mmol), 72 mg of $\text{Na}[\text{B}(\text{Ar}^{\text{F}})_4]$ (0.081 mmol), 21 mg of triphenylphosphine (PPh_3 , 0.080 mmol), and 20 mL of dichloromethane

were stirred for 2 h, at which point the mixture was filtered by cannula. The solvent was reduced to a minimal volume, and the concentrated solution was added slowly to chilled, rapidly stirred pentane (20 mL). The solid was isolated by cannula filtration and then dried under high vacuum overnight, yielding 98 mg of the yellow product (71%). Yellow crystals suitable for X-ray diffraction were grown by layering pentane on top of a concentrated solution of 13 in dichloromethane. Using Olex2,^{73a} the structure was solved with the XS structure solution program using the Patterson method and refined with the ShelXL refinement package using least-squares minimization.^{73b} Crystal data for C₈₀H₅₃BF₃₀IrN₂OP (*M*_r = 1862.51): triclinic, space group P $\bar{1}$ (No. 2), *a* = 12.7575(2) Å, *b* = 15.9555(2) Å, *c* = 37.5887(5) Å, α = 85.0951(7)°, β = 84.2762(7)°, γ = 81.0887(7)°, *V* = 7502.10(18) Å³, *Z* = 4, *T* = 100 K, μ (Cu *K*α) = 4.753 mm⁻¹, *D*_{calcd} = 1.649 g/mm³, 288052 reflections measured (2.368 ≤ 2θ ≤ 140.36), 27692 unique (*R*_{int} = 0.0395, *R*_σ = 0.0191), which were used in all calculations. The final *R*1 value was 0.0283 (*I* > 2σ(*I*)), and the w*R*2 value was 0.0680 (all data), with a goodness of fit on *F*² of 1.054. Anal. Calcd (found) for C₈₀H₅₃N₂BF₃₀IrOP: C, 51.60 (51.77); H, 2.87 (2.64); N, 1.50 (1.42). ¹H NMR (600 MHz, CD₂Cl₂): δ 8.21 (d, *J* = 7.8, 1H), 8.16 (d, *J* = 8.4, 2H), 7.96 (t, *J* = 7.2, 1H), 7.86 (d, *J* = 5.4, 1H), 7.72 (overlapping singlets, 10H), 7.63 (m, 2H), 7.59 (s, 1H), 7.56 (s, 4H), 7.57–7.52 (m, 4H), 7.46 (d, *J* = 7.8, 1H), 7.15 (t, *J* = 8.4, 2H), 7.06 (t, *J* = 7.2, 1H), 6.97 (t, *J* = 7.2, 1H), 6.77–6.74 (m, 3H), 6.60 (t, *J* = 6.0, 1H), 6.35 (d, *J* = 7.8, 1H), 5.98 (t, *J* = 9.0, 2H), 1.31 (s, 15H). ¹³C{¹H} NMR (150 MHz, CD₂Cl₂, one carbon merged to others): δ 171.3 (*J*_{C–P} = 2), 162.1 (1:1:1:1 quartet, *J*_{C–B} = 50), 158.1, 156.2 (*J*_{C–P} = 3), 146.9, 141.0, 138.3, 137.5 (*J*_{C–P} = 11), 135.1, 134.0 (*J*_{C–P} = 9), 132.9 (*J*_{C–P} = 9), 132.7 (*J*_{C–P} = 3), 132.4, 132.2 (*J*_{C–P} = 2), 131.9, 130.7, 130.5 (*J*_{C–P} = 2), 130.3, 129.8 (*J*_{C–P} = 10), 129.8 (q, 2-bond *J*_{C–F} = 35), 129.7, 129.2 (q, 2-bond *J*_{C–F} = 34), 128.9 (*J*_{C–P} = 11), 128.2 (*J*_{C–P} = 10), 127.0, 126.6, 125.5, 124.9 (q, 1-bond *J*_{C–F} = 271), 124.9, 124.3, 123.4 (q, 1-bond *J*_{C–F} = 271), 123.0 (septet, 3-bond *J*_{C–F} = 4), 117.8 (septet, 3-bond *J*_{C–F} = 4), 90.5 (*J*_{C–P} = 2), 9.8.

■ ASSOCIATED CONTENT

● Supporting Information

Figures, text, and CIF files giving NMR spectra of the OC and of new compounds, full structure reports, and detailed kinetic analysis. This material is available free of charge via the Internet at <http://pubs.acs.org>.

■ AUTHOR INFORMATION

Corresponding Author

E-mail for J.L.T.: joetemp@unc.edu.

Notes

The authors declare no competing financial interest.

■ ACKNOWLEDGMENTS

This research was supported by the UNC EFRC “Center for Solar Fuels”, an EFRC funded by the U.S. Department of Energy, Office of Science, Office of Basic Energy Sciences, under award DE-SC0001011. C.R.T. acknowledges support from the National Science Foundation Graduate Research Fellowship Program under Grant No. DGE-1144081 and from the National Science Foundation under Grant No. CHE-1058675.

■ REFERENCES

- (1) Nugent, W. A.; Mayer, J. M. *Metal-Ligand Multiple Bonds*; Wiley: New York, 1988.
- (2) (a) Holm, R. H. *Chem. Rev.* **1987**, *87*, 1401–1449. (b) *Biomimetic Oxidations Catalyzed by Transition Metal Complexes*; Meunier, B., Ed.; Imperial College Press: London, 2000. (c) Green, M. T.; Dawson, J. H.; Gray, H. B. *Science* **2004**, *304*, 1653–1656. (d) Rohde, J.-U.; In, J.-H.; Lim, M. H.; Brennessel, W. W.; Bukowski, M. R.; Stubna, A.; Münck, E.; Nam, W.; Que, L., Jr. *Science* **2003**, *299*, 1037–1039.

- (3) (a) Somorjai, G. A.; Li, Y. *Introduction to Surface Chemistry and Catalysis*; Wiley: Hoboken, NJ, 2010. (b) Rogal, J.; Reuter, K.; Scheffler, M. *Phys. Rev. B: Condens. Matter* **2007**, *75* (20), 205433. (c) Shelef, M. *Chem. Rev.* **1995**, *95*, 209–225. (d) Taylor, R. A.; Law, D. J.; Sunley, G. J.; White, A. J. P.; Britovsek, G. J. P. *Angew. Chem., Int. Ed.* **2009**, *48*, 5900–5903.

- (4) Poverenov, E.; Efremenko, I.; Frenkel, A.; Ben-David, Y.; Shimon, L.; Leitus, G.; Konstantinovski, L.; Martin, J. M. L.; Milstein, D. *Nature* **2008**, *455*, 1093–1096.

- (5) Efremenko, I.; Poverenov, E.; Martin, J. M. L.; Milstein, D. *J. Am. Chem. Soc.* **2010**, *132*, 14886–14900.

- (6) Hay-Motherwell, R. S.; Wilkinson, G.; Hussain-Bates, B.; Hursthouse, M. B. *Polyhedron* **1993**, *12*, 2009–2012.

- (7) Jacobi, B. G.; Laitar, D. S.; Pu, L.; Wargocki, M. F.; DiPasquale, A. G.; Fortner, K. C.; Schuck, S. M.; Brown, S. N. *Inorg. Chem.* **2002**, *41*, 4815–4823.

- (8) McGhee, W. D.; Foo, T.; Hollander, F. J.; Bergman, R. G. *J. Am. Chem. Soc.* **1988**, *110*, 8543–8545.

- (9) Cao, R.; Anderson, T. M.; Piccoli, P. M. B.; Schultz, A. J.; Koetzle, T. F.; Geletii, Y. V.; Slonkina, E.; Hedman, B.; Hodgson, K. O.; Hardcastle, K. I.; Fang, X.; Kirk, M. L.; Knottenbelt, S.; Kögerler, P.; Musaev, D. G.; Morokuma, K.; Takahashi, M.; Hill, C. L. *J. Am. Chem. Soc.* **2007**, *129*, 11118–11133.

- (10) Anderson, T. M.; Neiwert, W. A.; Kirk, M. L.; Piccoli, P. M. B.; Schultz, A. J.; Koetzle, T. F.; Musaev, D. G.; Morokuma, K.; Cao, R.; Hill, C. L. *Science* **2004**, *306*, 2074–2077.

- (11) Anderson, T. M.; Cao, R.; Slonkina, E.; Hedman, B.; Hodgson, K. O.; Hardcastle, K. I.; Neiwert, W. A.; Wu, S.; Kirk, M. L.; Knottenbelt, S.; Depperman, E. C.; Keita, B.; Nadjro, L.; Musaev, D. G.; Morokuma, K.; Hill, C. L. *J. Am. Chem. Soc.* **2004**, *127*, 11948–11949.

- (12) O'Halloran, K. P.; Zhao, C.; Ando, N. S.; Schultz, A. J.; Koetzle, T. F.; Piccoli, P. M. B.; Hedman, B.; Hodgson, K. O.; Boby, E.; Kirk, M. L.; Knottenbelt, S.; Depperman, E. C.; Stein, B.; Anderson, T. M.; Cao, R.; Geletii, Y. V.; Hardcastle, K. I.; Musaev, D. G.; Neiwert, W. A.; Fang, X.; Morokuma, K.; Wu, S.; Kögerler, P.; Hill, C. H. *Inorg. Chem.* **2012**, *51*, 7025–7031.

- (13) McDaniel, N. D.; Coughlin, F. J.; Tinker, L. L.; Bernhard, S. *J. Am. Chem. Soc.* **2008**, *130*, 210–217.

- (14) Dzik, W. L.; Calvo, S. E.; Reek, J. N. H.; Lutz, M.; Ciriano, M. A.; Tejel, C.; Hettterscheid, D. G. H.; de Bruin, B. *Organometallics* **2011**, *30*, 372–374.

- (15) Hettterscheid, D. G. H.; Reek, J. N. H. *Chem. Commun.* **2011**, *47*, 2712–2714.

- (16) Blakemore, J. D.; Schley, N. D.; Balcells, D.; Hull, J. F.; Olack, G. W.; Incarvito, C. D.; Eisenstein, O.; Brudvig, G. W.; Crabtree, R. H. *J. Am. Chem. Soc.* **2010**, *132*, 16017–16029.

- (17) Savini, A.; Bellachioma, G.; Ciancaleoni, G.; Zuccaccia, C.; Zuccaccia, D.; Macchioni, A. *Chem. Commun.* **2010**, *46*, 9218–9219.

- (18) Lalrempuia, R.; McDaniel, N. D.; Müller-Bunz, H.; Bernhard, S.; Albrecht, M. *Angew. Chem., Int. Ed.* **2010**, *49*, 9765–9768.

- (19) Miranda-Soto, V.; Parra-Hake, M.; Morales-Morales, D.; Toscano, R. A.; Boldt, G.; Koch, A.; Grotjahn, D. B. *Organometallics* **2005**, *24*, 5569–5575.

- (20) Hull, J. F.; Balcells, D.; Blakemore, J. D.; Incarvito, C. D.; Eisenstein, O.; Brudvig, G. W.; Crabtree, R. H. *J. Am. Chem. Soc.* **2009**, *131*, 8730–8731.

- (21) Zhou, M.; Schley, N. D.; Crabtree, R. H. *J. Am. Chem. Soc.* **2010**, *132*, 12550–12551.

- (22) Wang, C.; Wang, J.-L.; Lin, W. *J. Am. Chem. Soc.* **2012**, *134*, 19895–19908.

- (23) Zhang, T.; deKrafft, K. E.; Wang, J.-L.; Wang, C.; Lin, W. *Eur. J. Inorg. Chem.* **2014**, *2014*, 698–707.

- (24) Savini, A.; Belanzoni, P.; Bellachioma, G.; Zuccaccia, C.; Zuccaccia, D.; Macchioni, A. *Green Chem.* **2011**, *13*, 3360–3374.

- (25) Zuccaccia, C.; Bellachioma, G.; Bolaño, S.; Rocchigiani, L.; Savini, A.; Macchioni, A. *Eur. J. Inorg. Chem.* **2012**, *2012*, 1462–1468.

- (26) Junge, H.; Marquet, N.; Kammer, A.; Denurra, S.; Bauer, M.; Wohlrab, S.; Gärtner, F.; Pohl, M.-M.; Spannenberg, A.; Gladiali, S.; Beller, M. *Chem. Eur. J.* **2012**, *18*, 12749–12758.
- (27) Zhao, Y.; Hernandez-Pagan, E. A.; Vargas-Barbosa, N. M.; Dysart, J. L.; Mallouk, T. E. *J. Phys. Chem. Lett.* **2011**, *2*, 402–406.
- (28) Grotjahn, D. B.; Brown, D. B.; Martin, J. K.; Marelus, D. C.; Abadjian, M.-C.; Tran, H. N.; Kalyuzhny, G.; Vecchio, K. S.; Specht, Z. G.; Cortes-Llamas, S. A.; Miranda-Soto, V.; van Niekerk, C.; Moore, C. E.; Rheingold, A. L. *J. Am. Chem. Soc.* **2011**, *133*, 19024–19027.
- (29) Schley, N. D.; Blakemore, J. D.; Subbaiyan, N. K.; Incarvito, C. D.; D'Souza, F. D.; Crabtree, R. H.; Brudvig, G. W. *J. Am. Chem. Soc.* **2011**, *133*, 10473–10481.
- (30) Hintermair, U.; Hashmi, S. M.; Elimelech, M.; Crabtree, R. H. *J. Am. Chem. Soc.* **2012**, *134*, 9785–9795.
- (31) Zhou, M.; Hintermair, U.; Hashiguchi, B. G.; Parent, A. R.; Hashmi, S. M.; Elimelech, M.; Periana, R. A.; Brudvig, G. W.; Crabtree, R. H. *Organometallics* **2013**, *32*, 957–965.
- (32) Zhou, M.; Balcells, D.; Parent, A. R.; Crabtree, R. H.; Eisenstein, O. *ACS Catal.* **2012**, *2*, 208–218.
- (33) Zhou, M.; Schley, N. D.; Crabtree, R. H. *J. Am. Chem. Soc.* **2010**, *132*, 12550–12551.
- (34) Hintermair, U.; Sheehan, S. W.; Parent, A. R.; Ess, D. H.; Richens, D. T.; Vaccaro, P. H.; Brudvig, G. W.; Crabtree, R. H. *J. Am. Chem. Soc.* **2013**, *135*, 10837–10851.
- (35) Ingram, A. J.; Wolk, A. B.; Flender, C.; Zhang, J.; Johnson, C. J.; Hintermair, U.; Crabtree, R. H.; Johnson, M. A.; Zare, R. N. *Inorg. Chem.* **2014**, *53*, 423–433.
- (36) Graeupner, J.; Hintermair, U.; Huang, D. L.; Thomsen, J. M.; Takase, M.; Campos, J.; Hashmi, S. M.; Elimelech, M.; Brudvig, G. W.; Crabtree, R. H. *Organometallics* **2013**, *32*, 5384–5390.
- (37) Savini, A.; Bucci, A.; Bellachioma, G.; Rocchigiani, L.; Zuccaccia, C.; Llobet, A.; Macchioni, A. *Eur. J. Inorg. Chem.* **2014**, *2014*, 690–697.
- (38) Hettterscheid, D. G. H.; Reek, J. N. H. *Eur. J. Inorg. Chem.* **2014**, *2014*, 742–749.
- (39) Turlington, C. R.; Harrison, D. P.; White, P. S.; Brookhart, M.; Templeton, J. L. *Inorg. Chem.* **2013**, *52*, 11351–11360.
- (40) Macikenas, D.; Skrzypczak-Jankun, E.; Protasiewicz, J. D. *J. Am. Chem. Soc.* **1999**, *121*, 7164–7165.
- (41) Hupp, J. T.; Nguyen, S. T. *Chem. Eng. News* **2011**, *89* (2), 2.
- (42) (a) Song, F.; Wang, C.; Falkowski, J. M.; Ma, L.; Lin, W. *J. Am. Chem. Soc.* **2010**, *132*, 15390–15398. (b) Iwao, M.; Iihama, T.; Mahalanabis, K. K.; Perrier, H.; Snieckus, V. *J. Org. Chem.* **1989**, *54*, 24–26. (c) Clayden, J.; Cooney, J. A.; Julia, M. *J. Chem. Soc., Perkin Trans. 1* **1995**, 7–14.
- (43) At -70 °C, the singlet for the Cp* methyl groups in the ^1H NMR spectrum of the OC had decoalesced into two singlets, and a doublet assigned to an arylpyridine proton at 8.7 ppm had resolved into two doublets. The two isomers were present in roughly a 3:2 ratio.
- (44) Li, L.; Jiao, Y.; Brennessel, W. W.; Jones, W. D. *Organometallics* **2010**, *29*, 4593–4605.
- (45) Shaibu, B. S.; Kawade, R. K.; Liu, R.-S. *Org. Biomol. Chem.* **2012**, *10*, 6834–6839.
- (46) Campeau, L.-C.; Rousseaux, S.; Fagnou, K. *J. Am. Chem. Soc.* **2005**, *127*, 18020–18021.
- (47) Tan, Y.; Barrios-Landeros, F.; Hartwig, J. F. *J. Am. Chem. Soc.* **2012**, *134*, 3683–3686.
- (48) Kim, Y.-J.; Osakada, K.; Takenaka, A.; Yamamoto, A. *J. Am. Chem. Soc.* **1990**, *112*, 1096–1104.
- (49) Fu, R.; Bercaw, J. E.; Labinger, J. A. *Organometallics* **2011**, *30*, 6751–6765.
- (50) Miller, C. A.; Janik, T. S.; Lake, C. H.; Toomey, L. M.; Churchill, M. R.; Atwood, J. D. *Organometallics* **1994**, *13*, 5080–5087.
- (51) Dadci, L.; Elias, H.; Frey, U.; Hörnig, A.; Koelle, U.; Merbach, A. E.; Paulus, H.; Schneider, J. S. *Inorg. Chem.* **1995**, *34*, 306–315.
- (52) Theron, M.; Purcell, W.; Basson, S. S. *Acta Crystallogr., Sect. C* **1996**, *52*, 336–338.
- (53) Theron, M.; Basson, S. S.; Purcell, W. *Acta Crystallogr., Sect. C* **1995**, *51*, 1750–1752.
- (54) Fandos, R.; Walter, M. D. *Acta Crystallogr., Sect. E* **2006**, *62*, m264–m266.
- (55) (a) Su, T.; Lan, Y.-Q. *Acta Crystallogr., Sect. C* **2007**, *63*, m522–m524. (b) Chandler, B. D.; Cramb, D. T.; Shimizu, G. K. H. *J. Am. Chem. Soc.* **2006**, *128*, 10403–10412.
- (56) Zhou, Y.-H.; Fu, H.; Zhao, W.-X.; Tong, M.-L.; Su, C.-Y.; Sun, H.; Ji, L.-N.; Mao, Z.-W. *Chem. Eur. J.* **2007**, *13*, 2402–2409.
- (57) Ye, C.; Twamley, B.; Shreeve, J. M. *Org. Lett.* **2005**, *7*, 3961–3964.
- (58) (a) Lee, J. C.; Rheingold, A. L.; Muller, B.; Pregosin, P. S.; Crabtree, R. H. *J. Chem. Soc., Chem. Commun.* **1994**, 1021–1022. (b) Fairlie, D. P.; Woon, T. C.; Wickramasinghe, W. A.; Willis, A. C. *Inorg. Chem.* **1994**, *33*, 6425–6428.
- (59) Lee, E.; Hooker, J. M.; Ritter, T. *J. Am. Chem. Soc.* **2012**, *134*, 17456–17458.
- (60) Suess, A. M.; Ertem, M. Z.; Cramer, C. J.; Stahl, S. S. *J. Am. Chem. Soc.* **2013**, *135*, 9797–9804.
- (61) Sau, Y.-K.; Yi, X.-Y.; Chan, K.-W.; Lai, C.-S.; Williams, I. D.; Leung, W.-H. *J. Organomet. Chem.* **2010**, *695*, 1399–1404.
- (62) Hénanf, M. L.; Roy, C. L.; Pétilion, F. Y.; Schollhammer, P.; Talarmin, J. *Eur. J. Inorg. Chem.* **2005**, *2005*, 3875–3883.
- (63) Cross, J. L.; Garrett, A. D.; Crane, T. W.; White, P. S.; Templeton, J. L. *Polyhedron* **2004**, *23*, 2831–2840.
- (64) Thomas, S.; Lim, P. J.; Gable, R. W.; Young, C. G. *Inorg. Chem.* **1998**, *37*, 590–593.
- (65) The IR spectrum of $[\mathbf{1}][\text{SbF}_6]$ revealed a $\text{C}\equiv\text{N}$ stretch at 2258 cm^{-1} , which is indicative of a σ -bound NCAr^{F} nitrile ligand. The SbF_6 salt of $\mathbf{1}$ was used for IR studies because $\text{B}(\text{Ar}^{\text{F}})_4$ absorbs so strongly in the infrared region that the $\text{C}\equiv\text{N}$ stretch could not be identified. Note that the $\text{C}-\text{N}$ stretching frequency for π -bound nitrile ligands is dramatically lower, due to strong $d\pi-\pi^*$ orbital overlap.
- (66) Kukushkin, V. Y.; Pombeiro, A. J. L. *Inorg. Chim. Acta* **2005**, *358*, 1–21.
- (67) Macikenas, D.; Skrzypczak-Jankun, E.; Protasiewicz, J. D. *Angew. Chem., Int. Ed.* **2000**, *39*, 2007–2010.
- (68) Ryu, J.; Kwak, J.; Shin, K.; Lee, D.; Chang, S. *J. Am. Chem. Soc.* **2013**, *135*, 12861–12868.
- (69) (a) Glueck, D. S.; Wu, J.; Hollander, F. J.; Bergman, R. G. *J. Am. Chem. Soc.* **1991**, *113*, 2041–2054. (b) Yuan, J.; Hughes, R. P.; Rheingold, A. L. *Organometallics* **2009**, *28*, 4646–4648. (c) Sekioka, Y.; Kaizaki, S.; Mayer, J. M.; Suzuki, T. *Inorg. Chem.* **2005**, *44*, 8173–8175. (d) Kim, G. C.-Y.; Batchelor, R. J.; Yan, X.; Einstein, F. W. B.; Sutton, D. *Inorg. Chem.* **1995**, *34*, 6163–6172. (e) Yan, X.; Einstein, F. W. B.; Sutton, D. *Can. J. Chem.* **1995**, *73*, 939–955.
- (70) A reviewer suggested that the vacant coordination site on iridium could be filled by the oxygen atom of the benzamide. This would allow sPhIO to attack the carbonyl carbon of the benzamide and transfer an oxygen atom, forming an $\text{Ir}(\text{V})$ complex with a triply deprotonated, κ^3 -coordinated hydrated amide.
- (71) (a) Che, C.-M.; Ho, C.; Lau, T.-C. *J. Chem. Soc., Dalton Trans.* **1991**, 1901–1907. (b) Kojima, T.; Nakayama, K.; Ikemura, K.; Ogura, T.; Fukuzumi, S. *J. Am. Chem. Soc.* **2011**, *133*, 11692–11700.
- (72) Belal, R.; Meunier, B. *J. Mol. Catal.* **1988**, *44*, 187–190.
- (73) (a) Dolomanov, O. V.; Bourhis, L. J.; Gildea, R. J.; Howard, J. A. K.; Puschmann, H. *J. Appl. Crystallogr.* **2009**, *42*, 339–341. (b) SHELX: Sheldrick, G. M. *Acta Crystallogr., Sect. A* **2008**, *64*, 112–122.